

ENVIRONMENTAL DYNAMICS OF SURFACE WATER IN THE CARIBBEAN REGION

***Karl Heinz Szekiolda**

International Faculty Member, Ateneo de Manila University,

Department of Environmental Science

**Author for Correspondence: kszekiolda@ateneo.edu*

ABSTRACT

The major hydrographic features of the Caribbean Sea related to eddy propagation, upwelling and low salinity-water transport from the south are analyzed with averaged mapping, long-time series, of sea surface salinity, temperature and chlorophyll data. The analysis used the System for Multidisciplinary Research and Applications (Giovanni) and the Intra-Americas Sea Ocean Nowcast/Forecast System (IASNF). The data demonstrate the dynamics of the low salinity plume and its surface extension, during its transport from the Orinoco and Amazon estuaries to the Caribbean Sea. The salinity maximum in January coincides with the minimum discharge of the Orinoco and Amazon rivers. Separated patches of low salinity are visualized during August to September and seem to be jointly delivered by the outflowing water from the Amazon and the Orinoco effluents as recognized with salinity between 35.1 and 35.5 psu. By November, the southern part of the Caribbean Sea was seen to receive its freshwater input mainly from the Orinoco plume, however, it is evident that low-salinity water at this time is also generated through mixing with water from the Amazon plume. It was observed that this mixture might occasionally reach the coasts of Hispaniola and Puerto Rico. The distribution of salinity and sea surface height in the vicinity of the Lesser Antilles islands chain shows that destruction of rings may take place around 13⁰N and 15⁰N. Image interpretation shows that when cleaved surface portion of eddies pass through the island passages, they appear to reorganize back into anticyclonic rings. While the latitude zonal mean for salinity provides the averaged position of the major low salinity influx, image sequences show that freshened water can arrive in pulses and covers a wider longitudinal range that stretch from 11⁰N to 16⁰N with salinities < 33.5 psu. However, seasonal changes show that water approaching the Lesser Antilles is about 0.3 psu lower in salinity as compared to the eastern coasts of the Lesser Antilles. Variations, documented over the years, appear also in chlorophyll concentrations but were however not recognized in the data after 2010. Linear regression observed a temperature decrease in the vicinity of the Lesser Antilles of about 0.04⁰C y⁻¹. However, the polynomial fit indicated that a process with about a half-wavelength of ten years meanders through the region. A similar conclusion can be derived from the change in chlorophyll concentrations. A selected region in the Columbia Basin confirmed that the detected temperature anomalies around the Lesser Antilles were also recognized in the Columbia Basin with an increase in salinity and decrease in temperature for 2011 to 2014. The overall agreement is that regional trends in sea surface temperature in the wider Caribbean Sea during the latter half of 2000 to 2020 continued to increase but unevenly throughout the region. Averaged sea surface temperature increase for the wider Caribbean Sea is around 0.020⁰C y⁻¹ and may vary according to season from 0.017⁰C y⁻¹ to 0.024⁰C y⁻¹, but the Lesser Antilles showed a slight decrease of about 0.007⁰C y⁻¹. Although a negative temperature anomaly seems to persist after 2010, at the entrance of the Caribbean Sea, the effect of global warming is again recognized in the Columbia Basin in long-time temperature observations.

Keywords: *Salinity, Temperature, Chlorophyll, Sea Surface Height, Freshwater Transport*

INTRODUCTION

Understanding changes in the marine environment and particularly those in coastal and island regions would generate a better response to climate-related drivers. For instance, as a result of warmer sea surface

Research Article (Open Access)

temperature, mean water density in the upper 100 m has declined significantly by $0.02 \pm 0.003 \text{ kg m}^{-3} \text{ y}^{-1}$ (Taylor *et al.*, 2012). This change of hydrographic conditions has far reaching biological implications because primary production is affected when nutrient transport is modified. Sea level rise in the Caribbean Sea is similar to the global mean rise of approximately 1.8 mm y^{-1} while interannual mean sea level of the Caribbean region seems to be highly correlated with El Niño Southern Oscillation, but differences, however, are observed among Caribbean islands in the region where the trend is around 2 mm y^{-1} (Torres and Tsimplis, 2012). The barometric effect on coastal sea level during seasonal cycles in the Caribbean is insignificant annually but the seasonal cycle has large variations and peaks around October (Palanisamy *et al.*, 2012). Sea level rise is considered one of the most widely recognized climate change threats to low-lying coastal areas, and it is projected that global mean sea level increases by the year 2100 to 0.35 m to 0.70 m (Nurse *et al.*, 2014). Thus, a region like the Caribbean is exposed to an uncertain future vis-à-vis global change and related environmental deterioration. Environmental changes are recognized especially on islands and coastal areas in the Caribbean Sea with increasing surface air temperature and changes in minimum temperature that show stronger warming trends than maximum temperature. In addition, the frequency of extreme high temperatures has increased while fewer cool days, cool nights and extreme low temperatures were found (Stephenson *et al.*, 2014). It is in this connection that the objectives in the following study are to add to the existing knowledge of the Caribbean Sea and aim at contributing to a better understanding of the environmental complexity and changes of the region. The research addresses with image interpretation the major features that are associated with seasonal changes of water masses in the Caribbean Sea. Transport of water that contributes to low salinity in the Caribbean Sea will be shown for the period when sea surface salinity, temperature and chlorophyll data were available. In addition, longtime series were interpreted to recognize the trends with respect to global changes in temperature that are related to changes in the Caribbean Sea.

General overview of the Caribbean Sea

The Caribbean Sea is a semi-enclosed sea basin with the Greater Antilles in the north, and the Lesser Antilles in the east separate the Caribbean from the Atlantic Ocean. Geographically, Cuba, Hispaniola, and Puerto Rico are part of the Greater Antilles, while the smaller island group from Guadeloupe south to Grenada include the Lesser Antilles of which the northern segment of the Lesser Antilles are subdivided further into the Leeward Islands and the southern Windward Islands.

Due to the arid climate and low river discharge in the entire Caribbean, the water budget for the whole basin shows a water loss caused by an excess of evaporation over precipitation. The deficit in the water budget is compensated by the inflow of Atlantic water that enters from different passages, and estimates show that the origin is both in the North Atlantic and the South Atlantic Ocean, the latter having lower salinity and enters the Caribbean mostly through the southern passages with water from the North Atlantic entering as well through the southern passages. The Caribbean Sea has a complicated hydrography as very different water masses enter the sea and various processes contribute to the complexity. Speed and trajectories vary in different regions that indicate different mean flows and the action of eddies (Richardson, 2005). As seen in Figure 1, the Caribbean Current is the main current in the Caribbean Sea, and is basically an extension of the Guyana Current that flows into the Lesser Antilles and progresses along the northern coasts of South and Central America until it flows north into the Gulf of Mexico through the Yucatan Chanel. The major water transport through the Caribbean Current passes the Windward Islands Passages south of Guadeloupe at around 16.3°N to 61.5°W . The start of the Caribbean Current can be located at the region where tropical and South Atlantic waters enter the Caribbean Sea from the North Brazil Current.

The northeastern Caribbean Sea is not only under seasonal influence of the trade winds but also freshwater plumes from the Orinoco and the Amazon rivers that are responsible for the intensification of the Caribbean Current. Eddy activity in the northern part of the Caribbean Sea and low salinity plumes may even reach the vicinity of St. Croix in the United States Virgin Islands (Chérubin and Gravelli, 2016). Thus, the surface salinity layer in the Caribbean Sea is relatively low, with salinity values of <35.5 psu, as a result of mixing of North Atlantic surface waters, the Amazon and Orinoco river waters, and

Research Article (Open Access)

local freshwater runoff from South America. Hydrographic surveys indicate that water flows into the Caribbean Sea mostly through the Grenada, St. Vincent, and St. Lucia passages in the southeast (Gordon, 1967). The water then continues westward as the Caribbean Current that dominates the main surface circulation in the Caribbean Sea. Most of the transport into the Caribbean Sea occurs at depths shallower than 200 m (Carton and Chao, 1999). Two bands of flow are observed that enter the southeastern Caribbean Sea, and are located at around 12°N and 14°N and are separated by the islands between 12.0°N and 13.3°N. The northern inflow near 14°N is in the latitude range where rings from the north Brazil Current stall and decay east of the islands, and part of the inflow near 14°N appears to be deflected northward but merges with the main boundary flow near 66°W (Chérubin and Richardson, 2007).

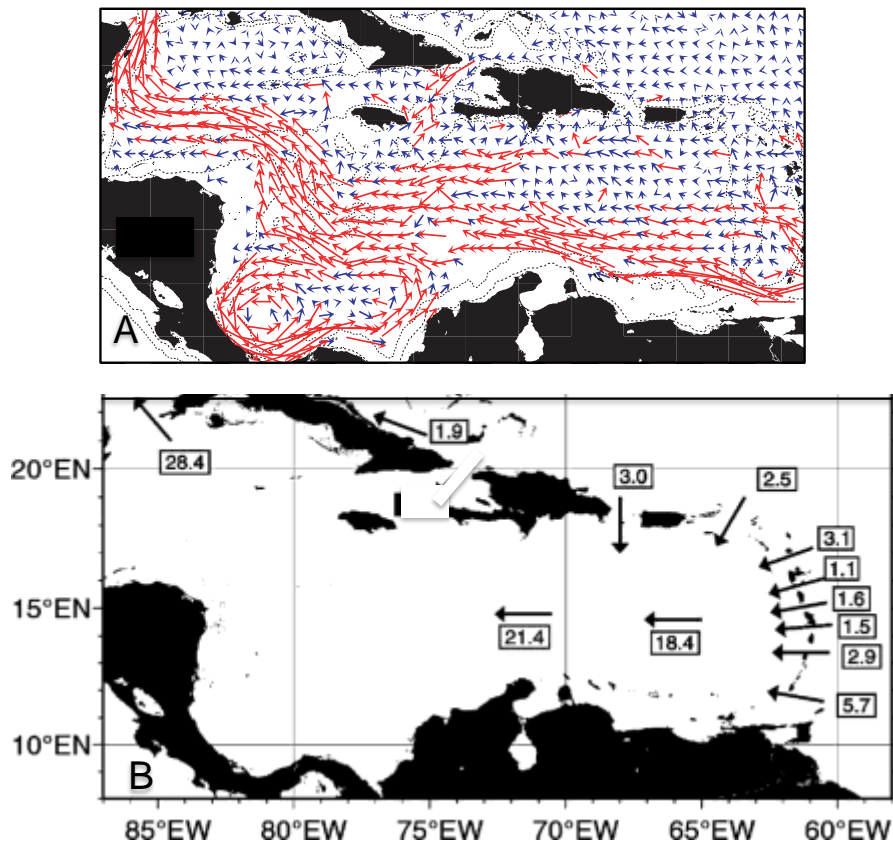


Figure 1: A: Mean velocity vectors and major transport modified from Richardson (2005). The westward flow of the Caribbean Current is shown by red vectors and included is the Panama–Colombia Gyre located in the southern Colombia Basin. B: Observed passage transport (Sv) after Johns *et al.* (2002).

The Caribbean Sea has a rather complicated hydrography through various passages as documented with estimates that are summarized by Gyory (2009), showing that the southern Lesser Antilles passages contributes about 22 Sv to the Florida Current (Schmitz and Richardson, 1991), while 7 Sv can be attributed to the Windward Passage further north (Johns *et al.*, 2002). Mean velocity vectors and major transport of the Caribbean Current are shown in Figure 1A and B. In general, water flowing into the Caribbean Sea is divided by the Windward Islands Passages south of Martinique, the Leeward Islands Passages between Martinique and the Virgin Islands and the Greater Antilles Passages between Puerto Rico and Cuba. It is estimated that water entering the Caribbean inflow is almost equally partitioned between the Windward, the Leeward, and the Greater Antilles Passages (Gordon, 1967). The surface flow is more complex around the Greater and Lesser Antilles because of a flow from the north into the

Research Article (Open Access)

Caribbean Sea near Puerto Rico and a more or less permanent eastward-flowing counter-current between Puerto Rico and Venezuela (Duncan *et al.*, 1982).

The Caribbean Current may reach a speed of 425 cm s^{-1} and at the opening, flows westward along the southern boundary of the Venezuela Basin near 12°N to 15°N , at a speed of approximately up to 80 cm s^{-1} . It reaches the center of the Colombia Basin through passages in the Jamaica Ridge where the current merges partly with the westward-flowing Panama–Colombia Gyre (Richardson, 2005). The major current enters the southern Caribbean Sea as a high-speed current and flows westward until it merges with the counterclockwise flow of the Panama–Colombia Gyre in the mid-Colombia Basin, while a second band of westward flow is in the northern Caribbean that also merges with the main southern current near 75°W (Richardson (2005). Eddies found in different parts of the Caribbean Sea translate with a similar mean velocity of local background flow that suggests that eddies are largely advected by the background flow and move westward at a speed of approximately 15 cm s^{-1} (Nystuen and Andrade, 1993). Those eddies progress westward to cross the basin within 180 days before dissipating near the coast of Nicaragua or the Yucatan peninsula (Carton and Chao, 1999). Anticyclones tend to appear in two bands, near 15°N and 17°N that are aligned with two jets of the Caribbean Current. The northern band was traced eastward to the Antilles where water enters from the North Equatorial Current and from North Brazil Current rings while the southern band was traced to the southeastern Caribbean where South Atlantic Water enters including some from North Brazil Current rings (Richardson, 2005). An estimate shows that about eight to nine rings may separate per year from the retroflexion and translate northwestward toward the Caribbean. From March to the end of the year, the retroflexion of the Brazil Current is well recognized and separated eddies from this region frequently entrain large volumes of the Amazon River water that drifts predominantly in anti-cyclonic motion with a warm core and mixes low-salinity river waters with the Atlantic surface water (Richardson (2005). South of 5°N , the water transport to the Caribbean is primarily of tropical and South Atlantic origin that crosses the equator in the North Brazil Current and flows in a northwest direction along the continental margin of South America as a coastal current, The North Brazil Current retroflects near 6°N and feeds into the eastward-flowing North Equatorial Countercurrent. At around 6°N , in the vicinity of the Amazon discharge area, the North Brazil Current curls into retroflexion generally from June to March and frequently dispatches eddies that progress in a northwestward direction in connection with the Guyana Current towards the Caribbean entrance, through passages between the Antilles Islands (Hellweger and Gordon 2002). Especially during the summer, eddies originating from the Brazil retroflexion zone arrive in the southern Caribbean, and propagation of mesoscale eddies dominates the physical dynamics and changes in productivity of the Caribbean Sea. A yearly cycle of rings is related to the strength of the North Brazil Current retroflexion and maximum transport is observed from July to December with its peak in September (Garzoli *et al.*, 2003). The North Brazil Current and its rings carry partly the nutrient load from the Amazon River and provide a mechanism for transport northwestward toward Tobago and Barbados (Müller-Karger *et al.*, 1988; Rueda-Roa and Müller-Karger, 2013). East of the Antilles, at around 14° to 18°N , the rings stall and may lose their characteristics after collision with the continental margin and the island chain (Johns *et al.*, 2002; Fratantoni and Richardson, 2006; Richardson, 2005). Ring fragments continue to migrate westward into the Caribbean as mesoscale eddies, and meander and travel along the Caribbean Current axis (Fu and Holt 1983; Andrade and Barton 2000; Fratantoni 2001; Van der Boog *et al.*, 2019). Detached freshened surface-water plumes may enter the southern Caribbean Sea south of Grenada Island while the northern inflow at 14°N passes the Grenadine Islands and St. Vincent (Chérubin and Richardson, 2007).

Two major upwelling regimes are located around Margarita Island in the Eastern Caribbean and in the Guajira region between about 61°W to 74°W and 10°W to 13°N (Rueda-Roa and Müller-Karger, 2013; Gomez Gaspar and Acero, 2020). The major cores of upwelling are from 63°W to 65°W , and towards the west, covers 70° to 73°W in the region of Colombian Guajira. Persistent trade winds in the eastern part of Venezuela cause Ekman transport and pumping offshore that decreases surface temperature by 1°C to 3°C . (Gomez Gaspar and Acero, 2020) with lowest surface temperature at around 25.2°C and maximum chlorophyll concentrations at around 1.7 mg m^{-3} . The corresponding temperature in the western

Research Article (Open Access)

region is 25.5°C and chlorophyll concentrations are at around 1.2 mg m^{-3} (Rueda-Roa and Müller-Karger, 2013). The origin of upwelled water can be found at a depth of about 120 to 40 m where the subtropical water ascends during the first months of the year with a salinity of about 36.9 psu. Variations in the upwelling system are at the mesoscale level, and the intensity of the upwelled water along the Guajira coast varies with the windforcing and is strongest in December-March and July, and weakest in the October-November rainy season (Gaspar and Acero, 2020). Anticyclonic gyres, that are formed in the eastern Caribbean Sea, intensify on their path westward while they pass the coastal upwelling region along the Venezuelan and Colombian coasts and transport low-salinity water from the Amazon and Orinoco River plumes. In addition, filaments of upwelled water transported offshore lead partially to cooling of the interior of the Caribbean Sea (Van der Boog *et al.*, 2019).

MATERIALS AND METHODS

Data sources

The study is primarily based on data processing via <https://giovanni.gsfc.nasa.gov/> and detail on the system are given by Acker and Leptoukh (2007). Resulting figures from this database will be referred to as Giovanni. The data in the system are derived from the MODIS instrument that has 36 spectral bands measuring reflection and emission between $0.405 \mu\text{m}$ and $14.39 \mu\text{m}$, respectively. The data are displayed in different formats as time-series and averaged maps for time-dependent events in selected study areas. Hovmöller plots were averaged over latitude and longitude for identifying with two-dimensional color graphs spatial-temporal changes. Three parameters were selected: a) sea surface daytime and nighttime temperatures measured at $11\mu\text{m}$, b) chlorophyll concentration and c) sea surface salinity.

The algorithm for chlorophyll in coastal waters and dense plankton blooms becomes uncertain especially in coastal areas where other non-living material interferes with the standard algorithm. However, in most oligotrophic waters in the Caribbean Sea as well as in the upwelling regions in the Caribbean, the algorithm is valid and the term chlorophyll is used with the understanding that data in the vicinity of river discharge regions refer more to ocean color rather than to a specific photosynthetic pigment.

In Giovanni sea surface salinity data are available only for the period September 2011 to May 2015, and therefore, specific salinity data only from that period are applied.

The Intra-Americas Sea Ocean Nowcast/Forecast System (IASNF) provides data in real time, and together with Giovanni data, aids in the interpretation with temperature and salinity measurements at 6km-resolution. Data are based on satellite altimeter and AVHRR measurements and were accessed at http://www7320.nrlssc.navy.mil/IASNFS_WWW/ that provides results from dynamical and statistical models together with oceanic observations and meteorological forcing to analyze sea surface elevation, ocean current, temperature, and salinity (Ko *et al.*, 2008). The used data are based on a data-assimilating ocean model (Martin, 2000) that continuously assimilates temperature and salinity, altimeter sea surface height anomaly from GFO, Jason-1, ERS-2 and thermal infrared sea surface temperature (Carnes *et al.*, 1996; Ko *et al.*, 2003; Rowley *et al.*, 2002). Furthermore, the system integrates climatology, temperature and salinity as inputs to estimate real-time salinity. The salinity data indicate real features but do not resolve accurately actual salinity differences around 0.2 to 0.4 psu (Fox *et al.*, 2002) but have a standard deviation of 0.22 psu (Chu *et al.*, 2004). Considering the salinity fluctuations in the investigated region over a range of about four salinity units, the IASNF provides sufficient resolution for recognizing salinity gradients and their dynamics.

Description of the selected test sites

Test sites have been selected based on anticipated dynamics and climatic surface features. The first is selected to generating an overview of the characteristics of the Caribbean Sea and the second test site refers to a region, where the major import of low-salinity surface water from the Atlantic and from the coastal regions of Brazil and Venezuela is observed. Sites 3 and 4 were chosen for identifying details on the pathway of freshened water from the Amazon and Orinoco Rivers and their flow through the passages of the Lesser Antilles to the Caribbean.

Research Article (Open Access)

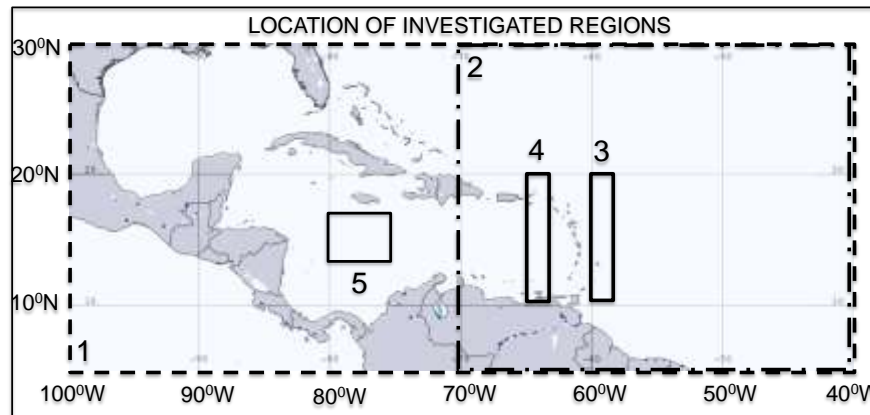


Figure 2: Location of investigated regions. Site 1 outer box: 5°N, 100°W to 30°N, 40°W; Site 2 covering the eastern part of the Caribbean and the Atlantic and the Amazon and Orinoco discharge area: 5°N, 70°W to 30°N, 40°W; Site 3: Entrance region of Atlantic water: 10°N, 60°W to 20°N, 58°W; Site 4: West of the Lesser Antilles: 10°N, 65°W to 20°N, 63°W; Site 5: Columbia Basin at 14°N, 80°W to 17°N, 75°W.

Site 5 is located in the Columbia Basin south of Jamaica, and the area was tested for detecting the amplitude of temperature changes in the central Caribbean Sea. An additional observation site in the vicinity of the Amazon discharge is located at, 0°N, 60°W, 15°N, 40°W, but it is not indicated in Figure 2.

RESULTS AND DISCUSSION

Average maps 2011 to 2015

Averaged maps do not resolve to a high degree dynamic features that are characteristic for the Caribbean Sea such as eddy propagation, upwelling and the transport of low-salinity water from the south. However, they provide means for recognizing the most important hydrographic features for more detailed analysis. This is shown with the surface temperature distribution in Figure 3 where the two major upwelling regions are recognized along the coastal regions of Columbia and Venezuela. The positions of the two cores of upwelling are located at 12°20'N and 71°57'W and around 11°N and 64°W.

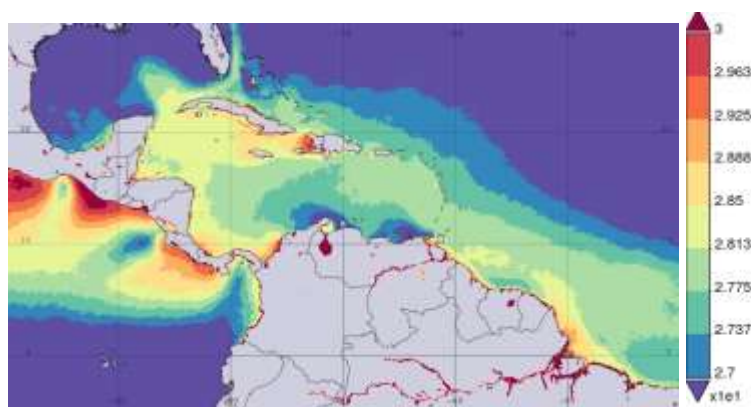


Figure 3: Time averaged map for surface temperature (°C) in the Caribbean region with data for all seasons from September 2011 to June 2015. The color bar on the right side of the image annotates temperature from 27°C to 30°C (Giovanni).

The spreading of water from the upwelling region is in a northwest direction but low temperatures are restricted mainly to the southern part of the Caribbean Sea while warmer water can be traced up to the

Research Article (Open Access)

Gulf of Mexico and finally to the Florida Strait. The influence of water from the deltaic region of the Amazon River is also recognized in the temperature field that shows slightly elevated values. However, the transport of freshened surface water from the Amazon and Orinoco rivers towards the Caribbean Sea is better recognized with the salinity distribution as shown in Figure 4. Although the averaged map with the low ground resolution does not allow a distinction between the Amazon and Orinoco discharge, it is evident that the major contributor to the low salinity at the entrance to the Caribbean is the Amazon effluent.

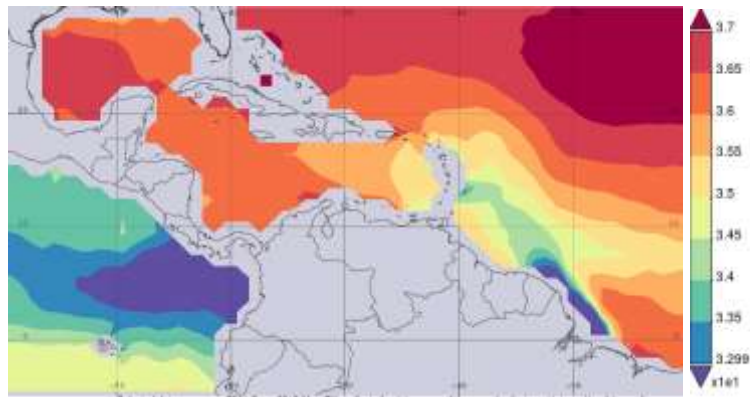


Figure 4: Time averaged map for salinity in the Caribbean region with data for all seasons from September 2011 to June 2015. The color bar on the right side of the image annotates salinity from 33.0 psu to 37.0 psu (Giovanni).

The low salinity plume from the Amazon River can be tracked along the South American coast up to where the river plume enters the passages of the Lesser Antilles, whereas another part of the low salinity plume extends east of the islands towards the Atlantic. Before entering the southern Caribbean Sea, the surface water still has a low salinity of around 34.0 psu to 35.45 psu. Temperature and salinity also define the biological system as is shown with the chlorophyll distribution shown in Figure 5. The Columbia and Venezuela coast upwelling regions are recognized by elevated chlorophyll concentrations. The effluent of the Amazon builds a strong boundary between the retroflexion of the Brazil Current and coastal water. However, for the interpretation of chlorophyll data, caution is needed because of the interference of chromophobic dissolved and solid substances that dominate the optical properties in coastal waters compared to the oligotrophic water in the Caribbean Sea.

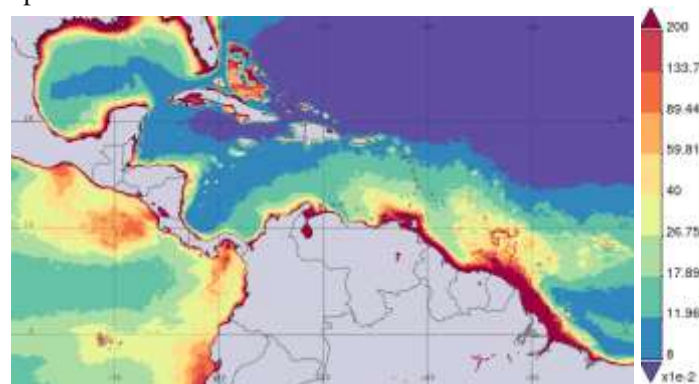


Figure 5: Time-averaged map for chlorophyll concentrations (mg m^{-3}) in the Caribbean region with data for all seasons from September 2011 to June 2015. The color bar on the right side of the image annotates chlorophyll concentrations from 0.08 to 2 mg m^{-3} on a logarithmic scale (Giovanni).

Research Article (Open Access)

Generally waters in upwelling areas have an inverse correlation of chlorophyll and temperature whereas regions exposed to freshwater discharge show a direct correlation with the chlorophyll signal and additional high content in chromophobic dissolved organic matter. This means that correlation between the two parameters may change from region to region according to their hydrological conditions, as is evident in Figure 6, where the correlation map shows the upwelling regions in the southern part of the Caribbean with a negative correlation between chlorophyll and temperature, whereas the river plumes from the Amazon and the Orinoco have a positive relation. A similar conclusion was derived by Rueda-Roa and Müller-Karger (2013) in the regions around the Orinoco River and other river discharge areas.

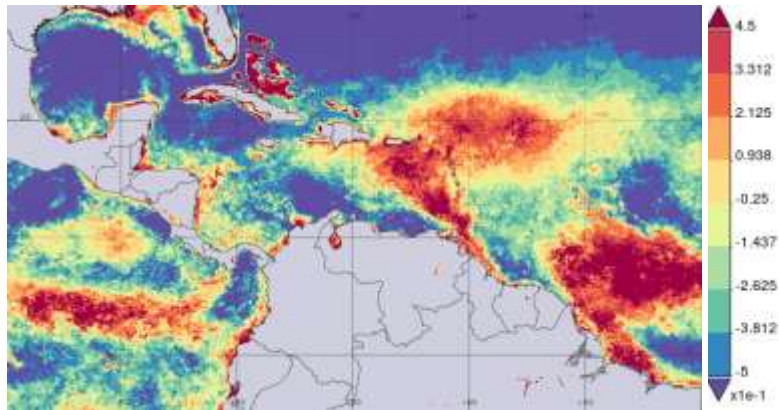


Figure 6: Temperature-chlorophyll correlation for September 2011 to February 2015 for Site 1, 5°S, 100°W to 30°N, 40°W with data for all seasons (Giovanni).

Positive correlation recognizes the different pathways of the Orinoco plume from the Amazon outflow; however, the Orinoco plume appears to pass through the southern passages of the Lesser Antilles only and reaches the Caribbean Sea as a mixture with other coastal waters. Two other regions appear isolated in the correlation map. One, is located northeast of the Amazon discharge region, and is interpreted as a region of eutrophication that is also connected to the retroflexion of the Brazil Current with a positive correlation. The other region that is characterized by a positive correlation is located north of the Antilles, but as indicated in Figure 5, is a region with low chlorophyll concentrations.

Seasonal changes in the Caribbean Sea

Seasonal changes in the Caribbean Sea are mainly an outcome of atmospheric variability and are dominated by the position of the Intertropical Convergence Zone that controls wind and precipitation conditions in the region (Poveda *et al.*, 2006). Thus, the Northern Trade Winds develop a rainy season from May to November and a dry season from December to April/June. An interim period shows reduced rainfall from July to August and is referred to as the mid-summer drought with significant spatial variability in timing and strength. The western Caribbean Basin receives a significant amount of freshwater from the Magdalena River and Atrato River (Restrepo and Kjerfve, 2000A), but the major contributor of freshwater to the Caribbean Sea, is the Amazon plume as can be seen with monthly salinity data for 2012 in Figure 7 that demonstrates the dynamics of the low salinity plume and its surface extension. The minimum freshwater transport to the Caribbean Sea is recognized in January when salinity has its maximum that coincides with the minimum discharge of the Orinoco and Amazon rivers. Starting in February, the decreasing salinity indicates increasing delivery of low salinity water especially from the Amazon effluent in isolated patches, and the impact of eddies is recognized at the beginning of March and April. During the period May to July, the surface salinity distribution shows the maximum extension of the Amazon plume and its transport towards the Caribbean Sea. Separated patches of low salinity are visualized during August to September that seem to be jointly delivered by the outflowing water from the Amazon and the Orinoco effluents and are best recognized with salinities between 35.1 and 35.5 psu.

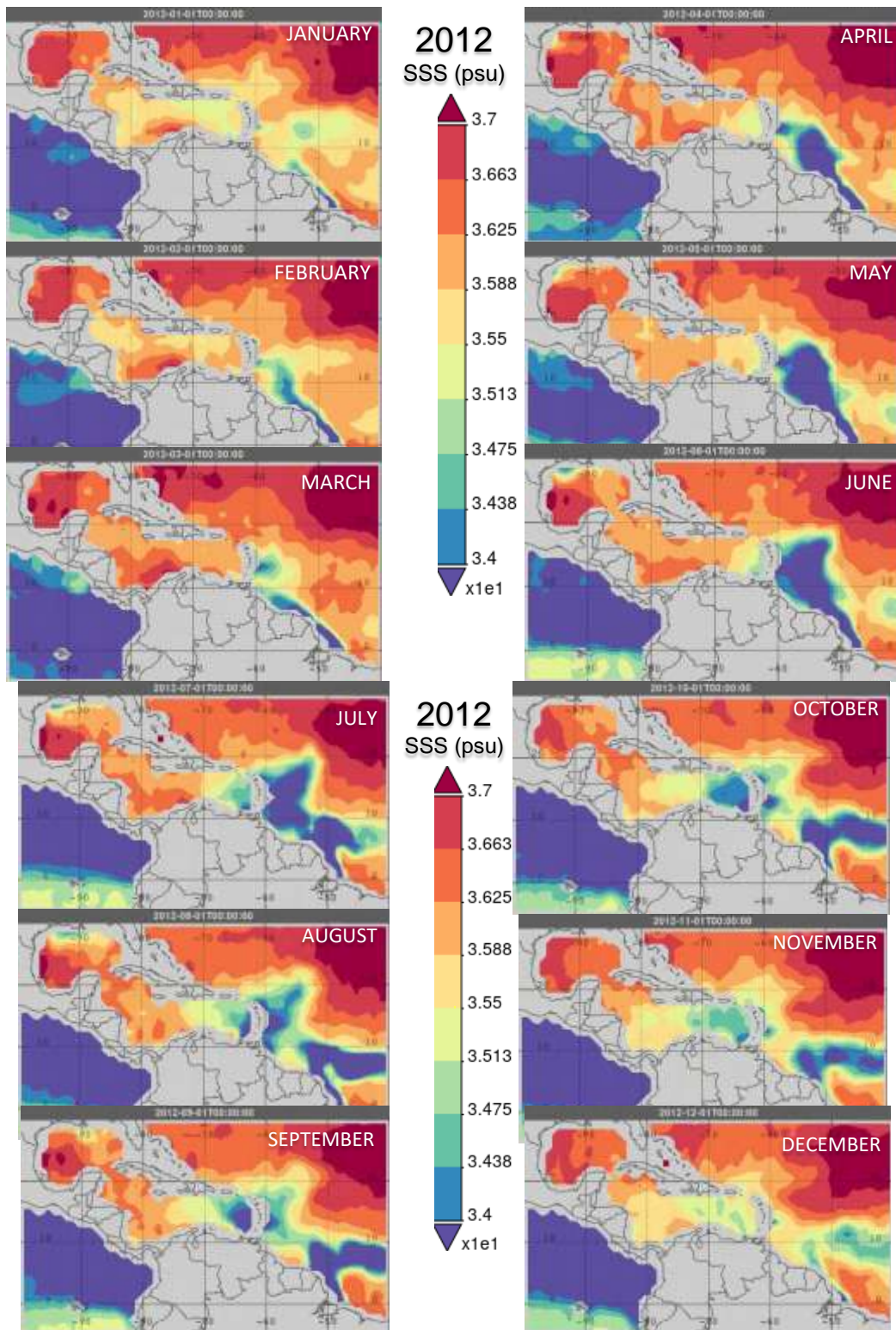


Figure 7: Monthly averaged salinity for 2012 at Site 1, 5⁰N, 100⁰W to 30⁰N, 40⁰W demonstrates the dynamics of the low-salinity plume towards the Caribbean Sea (Giovanni).

Research Article (Open Access)

Before reaching the passages of the Lesser Antilles, the Amazon plume deviates partly in a north direction that is documented for the period June to August. The Amazon effluent starts in July to move into an offshore direction in connection with the retroflexion of the North Brazil Current that is recognized until November. The images in Figure 7 document the seasonal changes with a minimal surface coverage of freshened water from January to March. In April, river discharge starts to advect the freshwater plume, as well as Orinoco water, towards the Caribbean Sea. The increased discharge is

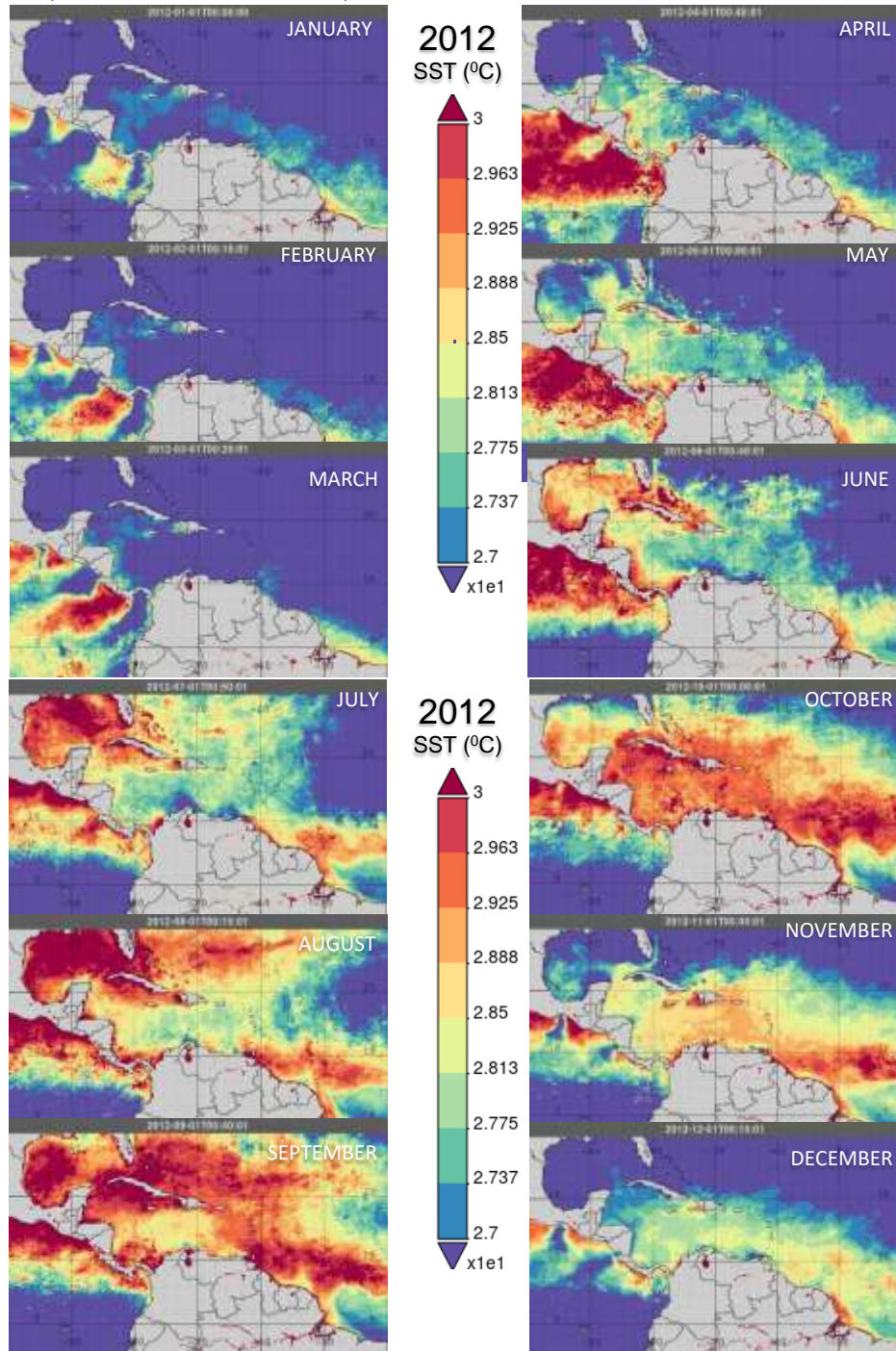


Figure 8: Monthly-averaged sea surface temperature for 2012 at Site 1, 5°N, 100°W to 30°N, 40°W (Giovanni).

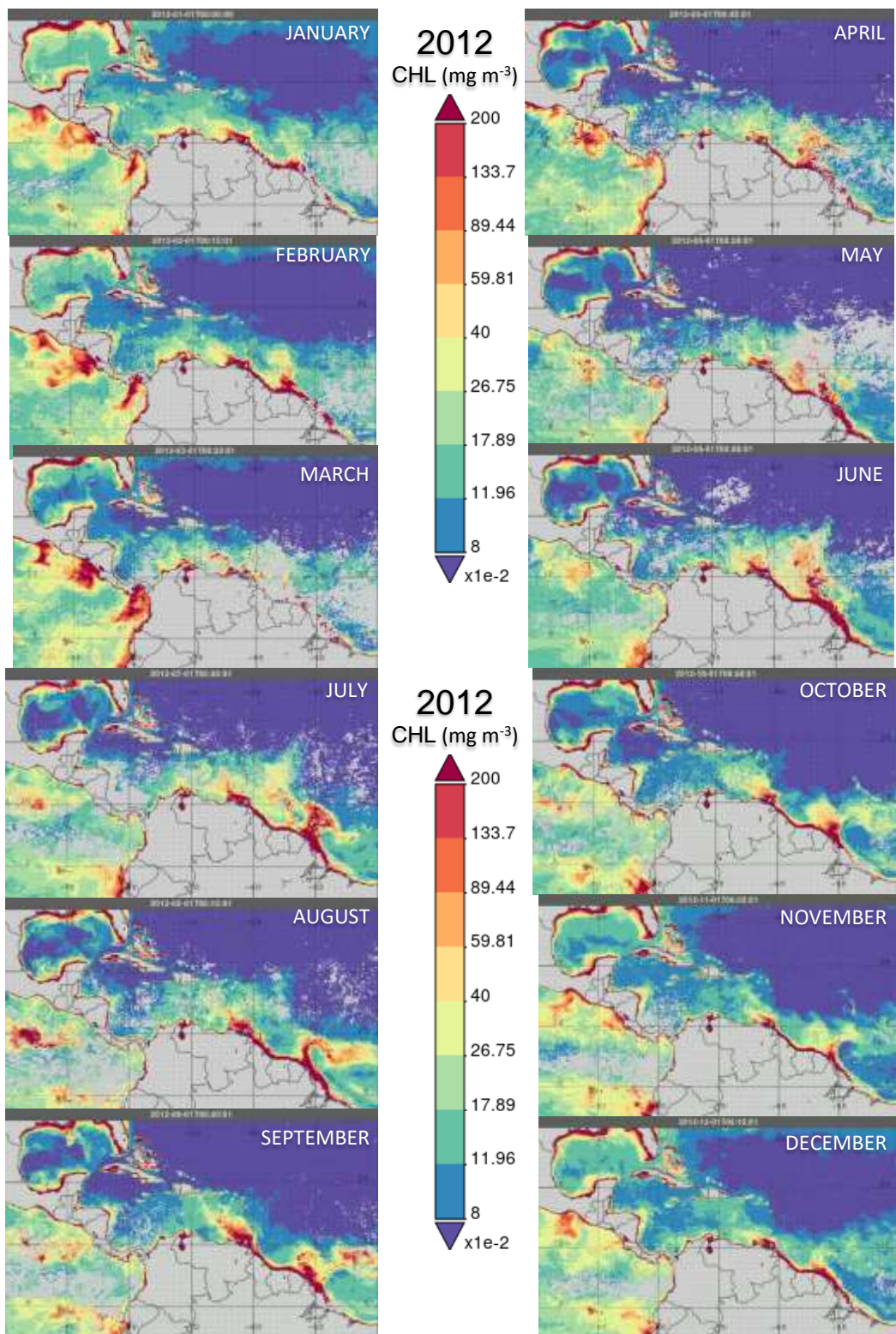


Figure 9: Monthly-averaged chlorophyll concentrations for 2012 at Site 1, 5°N, 100°W to 30°N, 40°W for 2012 (Giovanni).

recognized with the extended plume surface that progresses towards the north in June and July and for the rest of the year, isolated salinity patches indicate eddy building. The retroreflection of the North Brazil

Research Article (Open Access)

Current is also well recognized from August through December although the salinity increase in the retroflexion shows a decrease of freshwater supply to the region of retroflexion while the transport of freshened surface water to the Caribbean Sea appears also to be reduced.

These observations have to be viewed in relation to previous work on seasonal salinity changes. Especially in the eastern Caribbean Sea at 15°N, 65°W, highest salinity is found at around 36.1 psu in March and a minimum at around 34.5 psu in September/October, whereas near Grenada, where the Orinoco plume enters, higher variation of about 2.8 psu can be expected (Chérubin and Richardson, 2007). After the peak of seasonal rains in northeastern South America, the discharged water from the Amazon and Orinoco rivers extend northwestward across the Caribbean basin. During the pathway of the discharged water, salinity can range from 32 to 35 psu (Hu *et al.*, 2004), and the extension of the freshened water plume is recognized in Figure 7 with salinity of less than 34 psu. Although coarse, the resolution of the salinity data used in Figure 7 show the individual contribution of the Orinoco and the Amazon to the plume structure south of the Lesser Antilles.

Sea surface temperatures in Figure 8 show maxima in September/October around 29°C while minimum temperatures of less than 26°C are observed in February/March. The upwelling system in the southern Caribbean Sea is not well characterized with salinity data due to its rather low ground resolution of about 100 km and the small horizontal differences in concentration.

However sea surface temperature data shown in Figure 8 recognize in the southeastern Caribbean Sea the major upwelling around the coasts of Margarita Island, along the coasts of Venezuela and Guajira Peninsula and along the coast of Colombia that can be recognized from April to August. Both upwelling regions undergo strong spatial variability during the seasons. From January to March, no significant surface temperature gradients can be recognized but in April, when the southern part of the Caribbean Sea starts to warm, the two upwelling regions are recognized until July although horizontal temperature gradients are weak. In August, upwelling seems to cease but in December there is evidence of another upwelling event. Taylor *et al.* (2012) observed upwelling for the region to appear from December through May in response to trade wind intensification and shifting of the Intertropical Convergence Zone, but they also found that minor wind-driven upwelling events can occur in July to August, demonstrating that upwelling may appear seasonally and also aperiodically.

Changes in the strength of the North Trade Winds determine the nutrient transport from deeper water that lead to blooming in these regions (Torres, and Tsimplis, 2012; Morrison and Nowlin, 1982). However, almost no coastal upwelling was observed during the period July to November and blooms near the coasts can be increasingly rare in September and October (Müller-Karger *et al.*, 1988). Chlorophyll data in Figure 9 show a similar seasonal trend although the time frame for low upwelling activity in 2012 was indicated for August to December. The interpretation of upwelling in terms of chlorophyll concentrations is complicated because with the onset of increasing river discharge from the Orinoco River, the effect of plankton blooming through upwelling is partly masked by eutrophication from river effluents. Estimates for the Colombian upwelling transport show that it is about 1.5 times larger than in the eastern Venezuela upwelling because winds are about 1.3 times stronger (Andrade and Barton, 2000; Gomez Gaspar and Acero, 2020). Thus, the eastern part of the Venezuela upwelling reveals higher productivity because of upwelling subtropical subsurface water and nutrient transport from the low salinity water influx, mainly from the Orinoco and Amazon rivers. Surface transport of the Amazon plume is observed throughout the whole year but the retroflexion of the North Brazil Current, and associated offshore transport of Amazon water, is best recognized from July to November, and is also confirmed with the temperature measurements in Figure 8.

Flow of low-salinity water to the Caribbean Sea

The influx of freshened surface water into the Caribbean Sea has a maximum in spring and summer and a minimum in fall with a total range of about 4 Sv (Johns *et al.*, 2002). The extent of the freshwater plume relates to the seasonal discharge of the Amazon and Orinoco rivers when it spreads northwest towards the eastern Caribbean Sea starting in mid summer and continuing until October/November (Chérubin and Richardson, 2007). The Leeward Islands Passages have a maximum inflow in September and minimum in

Research Article (Open Access)

June but its cycle is nearly out of phase with that of the Windward Islands Passages (Johns *et al.*, 2002). This explains the high variability in the Caribbean Sea circulation as it is observed in both space and time. Some of it is based on mesoscale eddies and meanders that are related to wind forcing, bathymetry changes, current shear, and the occasional collision of water that arrives in the form of rings from the North Brazil Current. Because of their high discharge and northward transport, the Amazon and Orinoco rivers are the major contributors to the low-salinity water found in the southern Caribbean Sea. This is shown with the tremendous annual mean discharge rate of the Amazon River of about $1.9 \times 10^5 \text{ m}^3 \text{ s}^{-1}$ and the Orinoco River discharges about $3.1 \times 10^4 \text{ m}^3 \text{ s}^{-1}$ fresh water into the southern Caribbean Sea (Hu *et al.*, 2004). By comparison, the total annual mean discharge of local rivers in the Columbian Basin is approximately the equivalent to about 50 percent of the annual mean discharge of the Orinoco River into the eastern Caribbean Sea (Beier *et al.*, 2017).

The plume from both the Orinoco and Amazon extends in a northwest direction but the Amazon plume arrives, with a delay of three to four months at the entrance to the Caribbean basin south of Grenada. A northern inflow to the basin is observed at 14°N and passes northward around the Grenadine Islands and St. Vincent (Richardson, 2005; Fratantoni and Richardson, 2006; Chérubin and Richardson, 2007; Duncan, *et al.*, 1982). Although the river discharge of the Orinoco is significant and closer to the Caribbean Sea, the Amazon River dominates the impact on the salinity budget in the Caribbean Sea (Müller-Karger *et al.*, 1988). There is also a time difference between the maximum discharges of both rivers because the maximum discharge of the Amazon is around May/June, whereas the maximum for the Orinoco discharge is around August. That means that at a certain time of the year, both plumes arrive at the Lesser Antilles with the same intensity whereas at other times, one or the other dominates with freshwater supply. For instance, Figure 10 shows that in December the Orinoco plume, although not at its discharge peak, dominates the freshwater supply at the entrance to the Caribbean Sea.

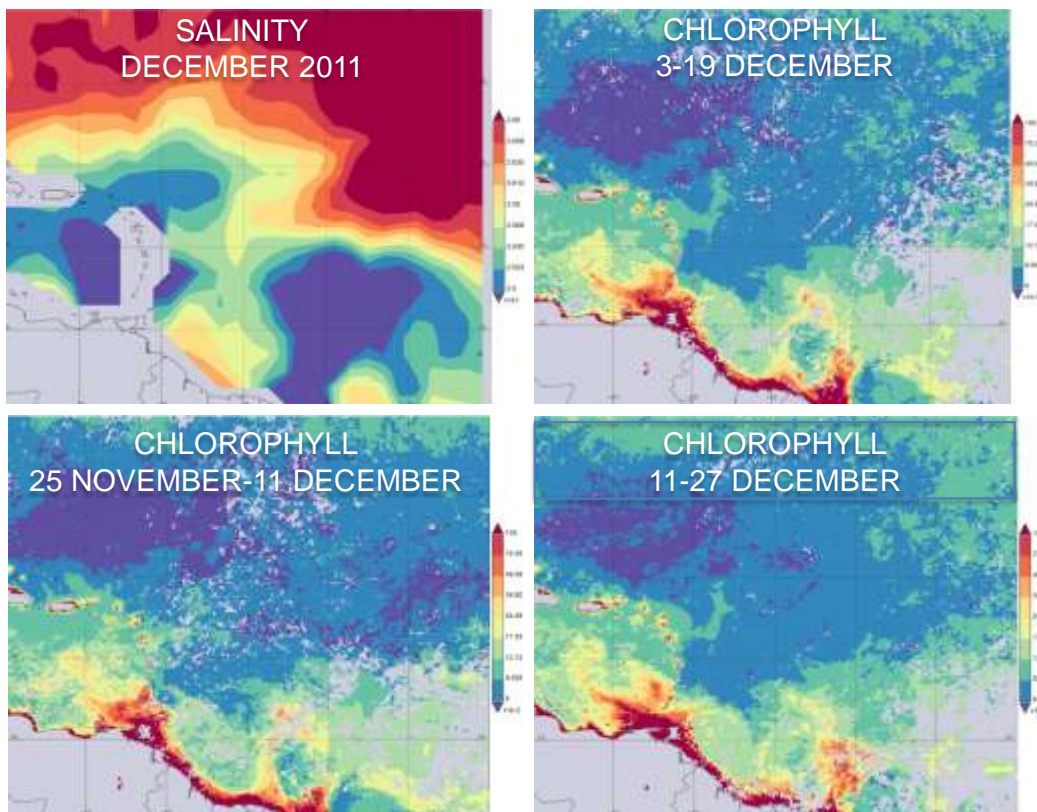


Figure 10: Monthly averaged salinity distribution for December 2011. The sequence of chlorophyll estimates is based on two-weekly averaged values (Giovanni).

Research Article (Open Access)

The influence of freshwater from the Amazon and the Orinoco rivers is recognized with salinities <35 psu, but water with >35.0 and <35.7 psu shows that the whole area is induced by both effluents. A similar distribution pattern is observed with chlorophyll concentrations that are shown as a sequence of two-weekly averaged values in Figure 10. Two major regimes can be seen that are defined by elevated chlorophyll concentrations. The Amazon region shows offshore transport, and eddy propagation and chlorophyll values > 0.17 mg m⁻³ connect the eutrophic effect of both river plumes that was also documented by Müller-Karger et al. (1989) who showed that the pigment plume of the Orinoco River expands towards the Caribbean Sea to about 3x10 km² and can reach Puerto Rico around September/October. Discharged water from the Orinoco River is recognizable in the southeastern Caribbean Sea with low salinity plume close to the coast, but the dispersal from the discharge region to the entrance of the Caribbean Sea is difficult to recognize because of the low signal difference between the Amazon plume and the discharged water from the Orinoco River.

The interpretation of daily IASNF-salinity distribution shows that in July–August, a mixture of the Amazon and Orinoco freshwater plumes extends northwest across the eastern Caribbean Sea. However, the Amazon water travels nearly 2000 km to reach the Caribbean Sea whereas the Orinoco River travels only about 300 km and arrives in the Caribbean Sea within ten days. By September, both plumes are separated over a short distance and it seems that by November, the southern part of the Caribbean Sea receives its major freshwater input mainly from the Orinoco plume. This is also indicated by the entrance of the Orinoco plume into the Caribbean Sea having a similar seasonal pattern of discharge, although a two-month lagged Amazon discharge was observed (Hellweger and Gordon, 2002; Chérubin and Richardson, 2007). The salinity distribution in Figure 11 for December provides coverage of salinity distribution that reveals that the Orinoco plume is rather limited in its expansion. However, the effluent has a strong optical signature that is based on high concentrations of chromophobic dissolved organic matter (CDOM) and high discharge of sediments compared to other coastal regions (Odriozola *et al.*, 2007).

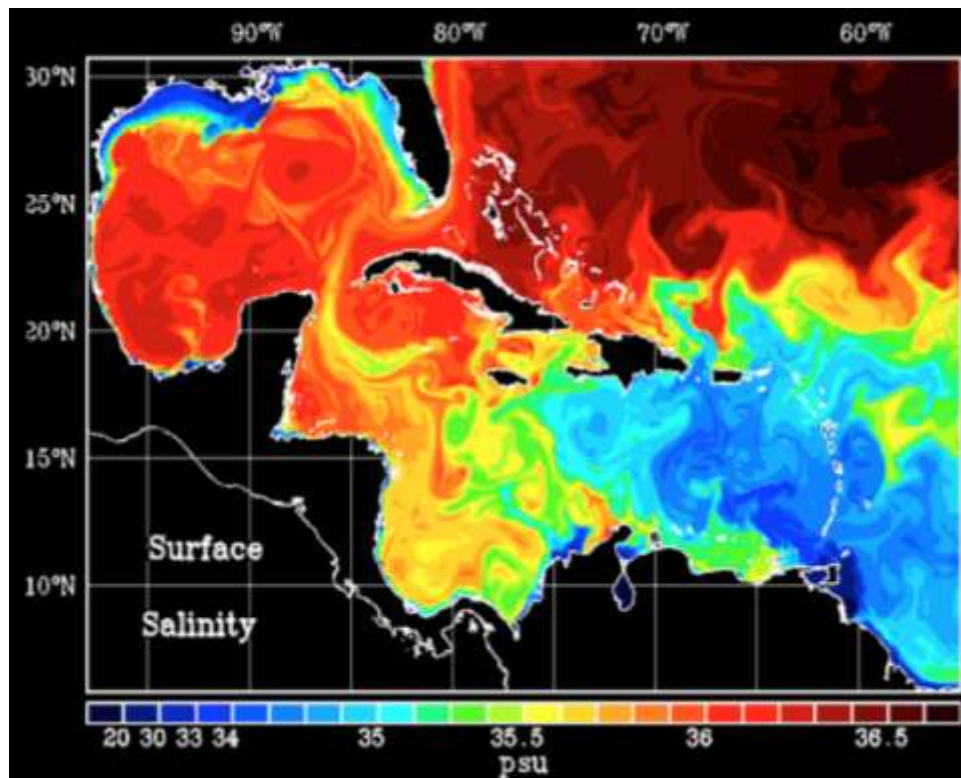


Figure 11: Salinity distribution showing the Orinoco plume and freshened water from the Amazon on 7 December 2011 (IASNF).

Research Article (Open Access)

Interpretation of daily coverage IASNF-videos showed that the mixture of Orinoco and Amazon plume-water might occasionally reach through filaments the coasts of Hispaniola and Puerto Rico. However, from December to January, the Orinoco plume is recognized in images as a separate outflow with an adjacent salinity of about 35.2psu, mixing rather quickly downstream with low-salinity water from the Amazon plume. The salinity distribution in Figure 11 implies that the plume structure is solely derived from Orinoco and Amazon water. However, comparing the daily sequence of salinity in December reveals that the pathway of the Orinoco plume is rather restricted because the Orinoco plume during its northwest movement is also mixed partially with upwelling that appears along the northern coast of Trinidad and Tobago. This is demonstrated with the average temperature and chlorophyll concentrations in Figure 12 that shows significant local upwelling along the coast of Trinidad that may have been unnoticed in previous studies.

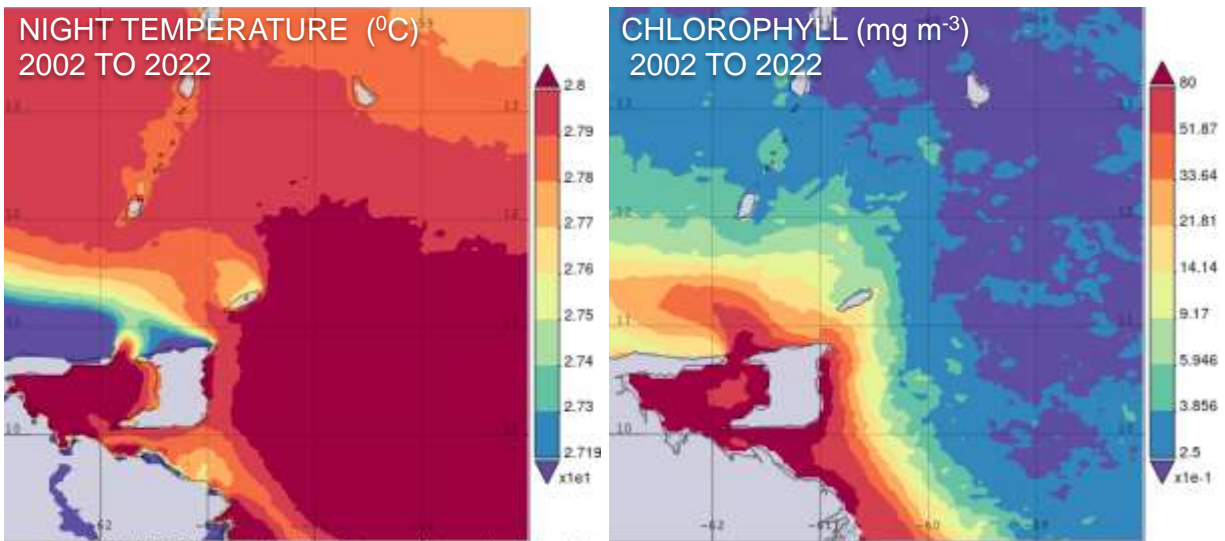


Figure 12: Averaged temperature and chlorophyll distributions for 2002 to 2022 to show the impact of upwelling along the coast of Trinidad and Tobago (Giovanni).

Seasonal changes of current patterns, fluctuations in the retroflection, and wind changes complicate the interpretation of seasonal variability in the Amazon and Orinoco plumes. Therefore, it has been difficult to distinguish the relative contributions of both rivers downstream to the surface salinity. Since the Orinoco River discharge is close to Barbados and to the entrance of the Caribbean Sea, seasonal changes in river discharge of the Orinoco plume are inversely related to the salinity off Barbados. However, taking into account the discharge volume of the Orinoco and the Amazon rivers, it shows that only 15 percent of the two-month lagged Amazon is required to account for the salinity decrease in Barbados (Hellweger and Gordon 2002). On the other hand, the low salinity water observed in the northern Caribbean Sea is assumed to be dispersed Orinoco river water because the water offshore in the Caribbean shows higher concentrations of silica than the low-salinity water drifting east of the Antilles (Müller-Karger, *et al.*, 1989).

Transport of low-salinity water through the Lesser Antilles passages and eddy activity

In the Lesser Antilles region, the main transport of water into the Caribbean Sea is through the passages along Grenada, St. Vincent, and St. Lucia and the water moves westward as the Caribbean Current (Gyori *et al.*, 2009). As rings from the retroflection of the North Brazil Current transport low salinity water downstream, they are modified by interaction with other neighboring rings and in particular, through contact with the bathymetry along the continental shelf of South America. Once they arrive at the low bathymetry close to the Lesser Antilles island chain, they are forced in a northward direction. At the

Research Article (Open Access)

latitude of Tobago, a separation of rings may take place that establishes upper and lower parts of which the shallow part may propagate further northwestward, while the deeper part remains near Tobago and possibly interacts with subsequent rings (Fratantoni and Richardson, 2006). After stalling, the rings may also integrate at the islands into streamers and propagate north of Barbados up to 16°N (Jochumsen *et al.*, 2010). These processes can explain that streamers clear through the Lesser Antilles Islands Passages and are responsible for eventually inducing new anticyclonic and cyclonic ring formations in the eastern Caribbean Sea (Richardson, 2005). The decay of eddies in the vicinity of Barbados is connected to the cleaving of the near-surface and sub-thermocline structures. Thus, the North Brazil Current rings do not appear to pass the island passages as whole rings (Fratantoni and Richardson, 2006). As the cleaved surface fraction retains its ring-like circulation, it is important to understand the progression of the surface water through the passages of the Lesser Antilles and into the eastern part of the Caribbean Sea. For this purpose, a sequence of surface salinity and sea surface height measurements will be used to elaborate on surface features that can be recognized in surface data. The analysis is based on IASNF data sets comparing of sea surface salinity and sea surface height.

A sequence of salinity distribution with corresponding sea surface heights is shown in Figure 13 for 1 April to 25 May. In general, the Caribbean Current is well recognized and the elevated surface height in the north is observed in the area of the Greater Antilles, whereas the southern part of the Caribbean Sea is dominated by low elevation that signifies the position of the two upwelling areas along the Colombian and eastern Venezuela coasts.

At the entrance to the Caribbean Sea, low-salinity water approaches the Lower Antilles passages and surface water disperses through the island channels as can be recognized with the filaments detached from the major plume. Although the salinity minimum carries the signature of an approaching eddy on 3 April, the surface height does not indicate eddy appearance except for a slight elevation that coincides with the location of the salinity minimum and can be tracked in a northwest direction. On 7 April, the dispatch of filaments continues and the main water body diverts in a northwest direction east of the Lesser Antilles. 7 April shows increasing sea surface height that becomes stronger on 13 April, while the salinity plume starts to disintegrate at the northern border into a diffuse pattern between 10°N and 15°N.

The elevated sea surface height coincides with the position of the minimum salinity values and shows that the intrusion of low salinity water translates earlier than the elevated water mass that seems to be a sign of ring separation due to interaction of an eddy with the bathymetry, a process that was described by Fratantoni and Richardson (2006) as cleaving of surface and subsurface portions of rings. This process separates an eddy in two sections at a depth of about 200 to 300 m with each portion retaining a coherent, independent and ring-like vertical circulation.

Cleaving of surface and subsurface portions of rings seems to start early April when parts of the freshened water are partitioned by the island chain while part of the water mass with minimum salinity stays isolated on the eastern side of the island chain but continues to spread in a northeast direction. Water with the lowest salinity appears as a ring-like structure that is also recognized as an area of elevated surface height. The diffuse pattern in surface height is an indication that residual parts of an eddy around 13°N and 15°N pass through the Lesser Antilles passages close to the island of St. Lucia. Following this development on 15 May and 20 May, as shown in Figure 13, minimum salinities still appear in the same location but water with higher surface elevation seems to be indicative for an advancing eddy. This is evidenced with the sequence of images for 22 May and 25 May, the latter showing water with low salinity and an indication of an eddy approaching the island chain. This eddy stalls until 7 June in the same location as seen in Figure 14 by the augmented surface elevation.

As the Lesser Antilles are the major obstacle for westward movement of rings, the transfer of water entering into the Caribbean Sea undergoes a mechanism that includes the destruction of rings through scraping against the corrugated boundary of the island chain, a process that was cited by Fratantoni and Richardson (2006). Furthermore, cleaving and shoaling of eddies seem to be prompted prior to the arrival of eddies at Barbados. Thus, ring water is redistributed and is transferred in discrete packages through the island passages in the form of filaments whose size is determined by the width of the island passage.

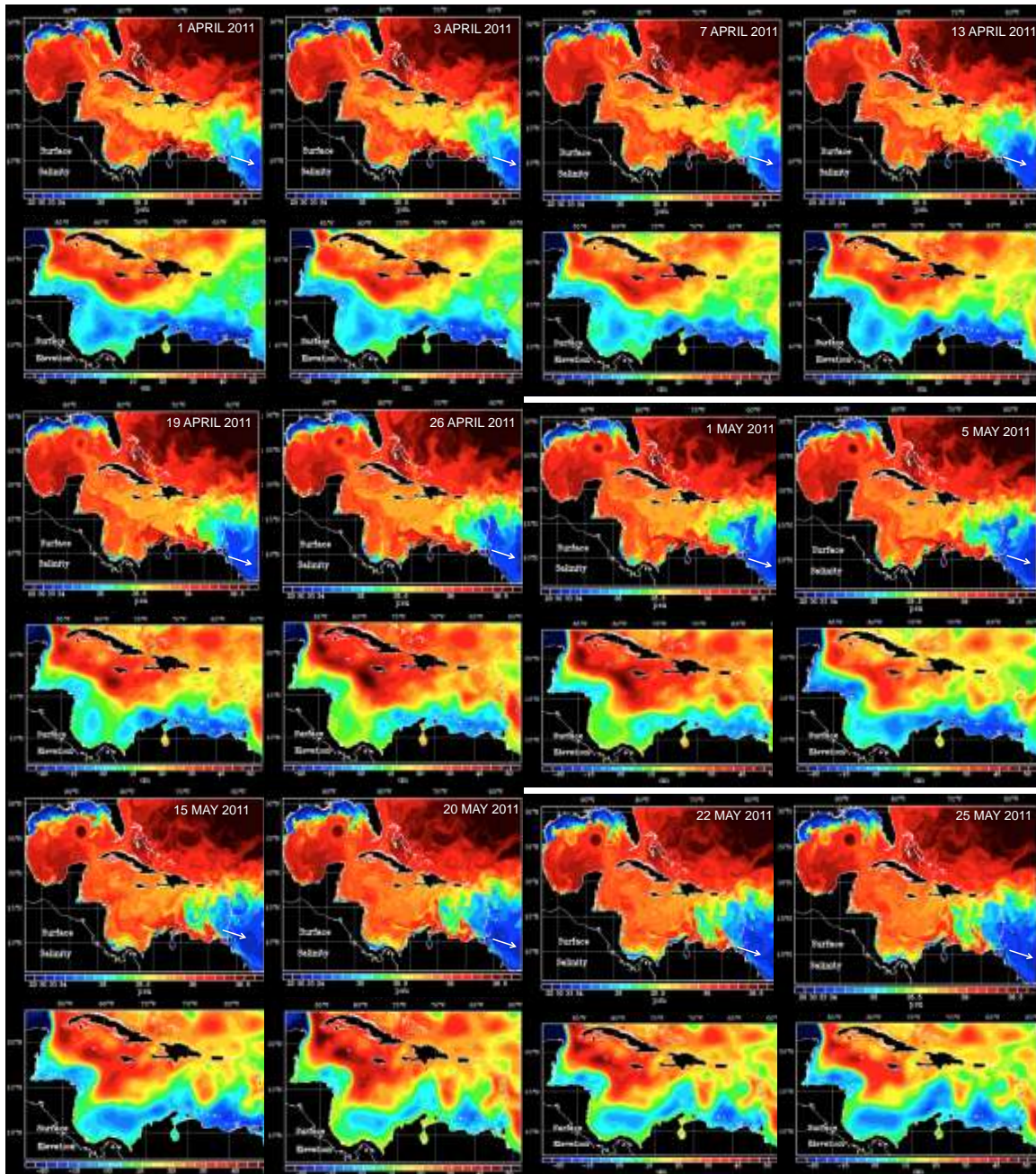


Figure 13: Comparison of sea surface salinity and sea surface height from 1 April to 25 May 2011. Upper images show the salinity distribution and below are the corresponding images for sea surface height for the same dates. Arrows in the salinity images identify the locations of minimum salinity (IASNF).

Under the assumption that elevated surfaces progressing from southeast are indicators for eddy presence, the sequence of images showed their dispersal during their approach to the Lesser Antilles.

Research Article (Open Access)

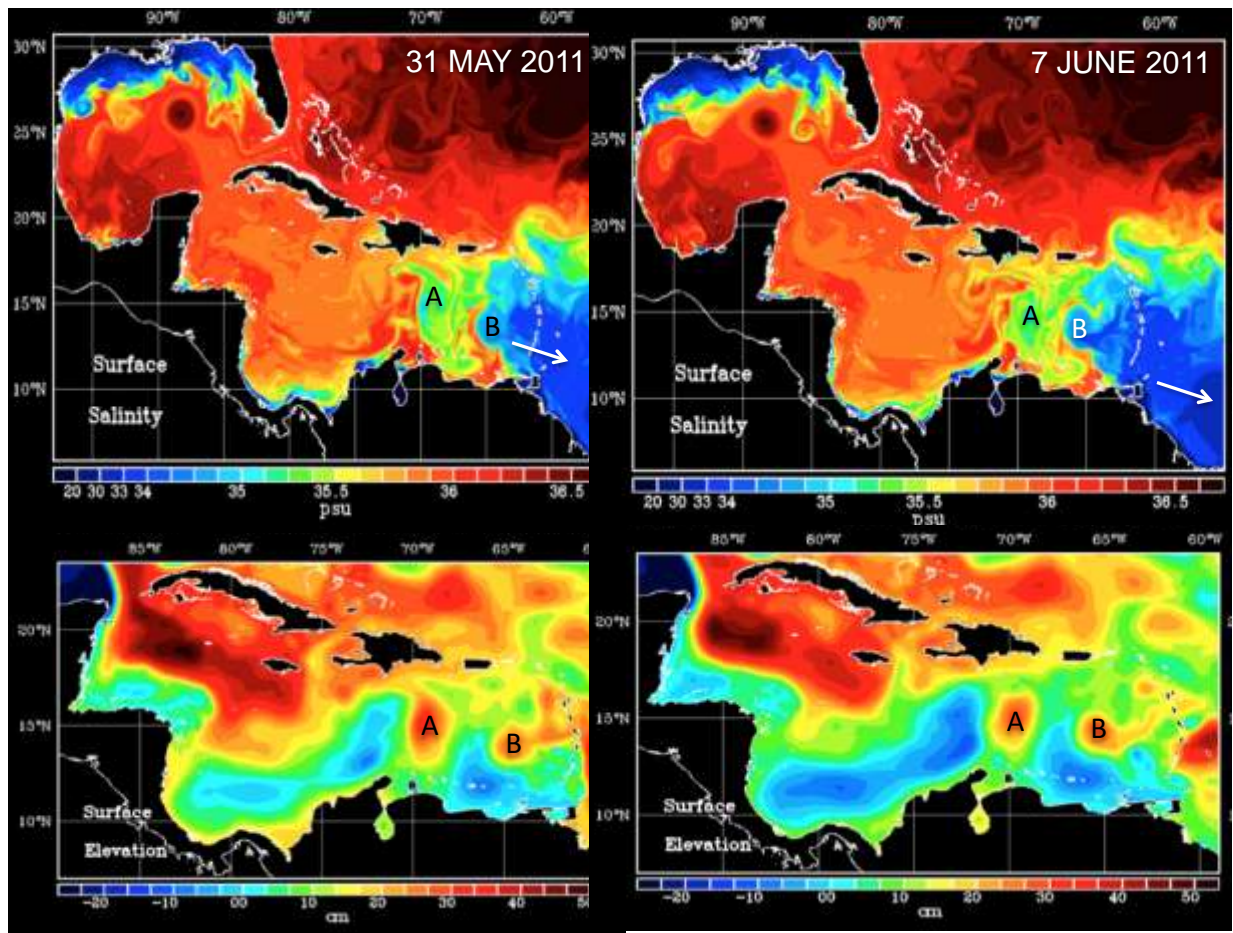


Figure 14: Comparison of surface salinity sea and surface elevation for 31 May and 7 June 2011 (IASNF).

The images in Figure 14 for 31 May and 7 June show that once the cleaved surface portions pass through the passages, they appear to reorganize back into anticyclonic rings and progress westward with increasing surface heights that indicate strengthening. At the start, the new rings are constructed at the western part of the islands with low salinity water from the Orinoco and Amazon rivers. Further westward, the rings also incorporate at the outer edge, filaments from the upwelling regions, as shown in Figure 14 with rings A and B while another ring approaches the island chain from the east. On 13 and 20 June, a dissected ring passes the islands and a new eddy is reconstructed that is recognized by salinity and surface height around 23 to 30 June, as seen in Figure 15. Based on daily IASNF coverage, the detected eddies show anticyclonic rotation and continue to migrate westward through the Caribbean Sea.

The sequence of salinity and sea surface height observations shows that the passages at the Lesser Antilles play the major role in regulating the flow of low salinity to the Caribbean Sea but the flow of water to the entrance of the Caribbean Sea also undergoes seasonal cycles. For instance, the Leeward Island Passage has maximum inflow in September and minimum in June, but its cycle is nearly out of phase with that in the Windward Islands passage (Johns *et al.*, 2002). The effect of seasonal changes is also recognized in the latitude averages for salinity as is shown with Hovmöller longitude averaged salinity, chlorophyll and temperature data in Figure 16.

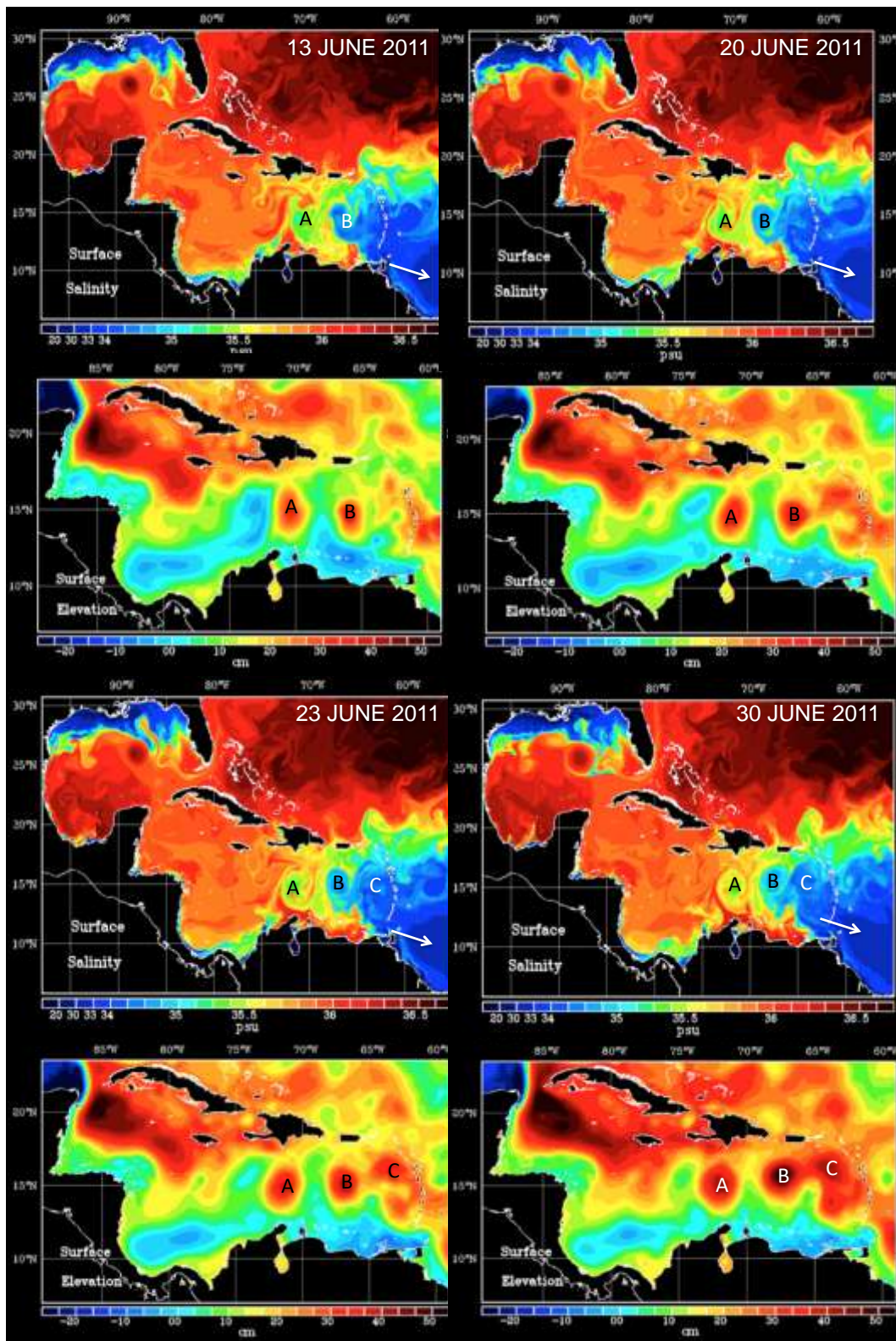


Figure 15: Comparison of surface salinity sea and surface elevation for 23 June to 30 June 2011 (IASNF).

Research Article (Open Access)

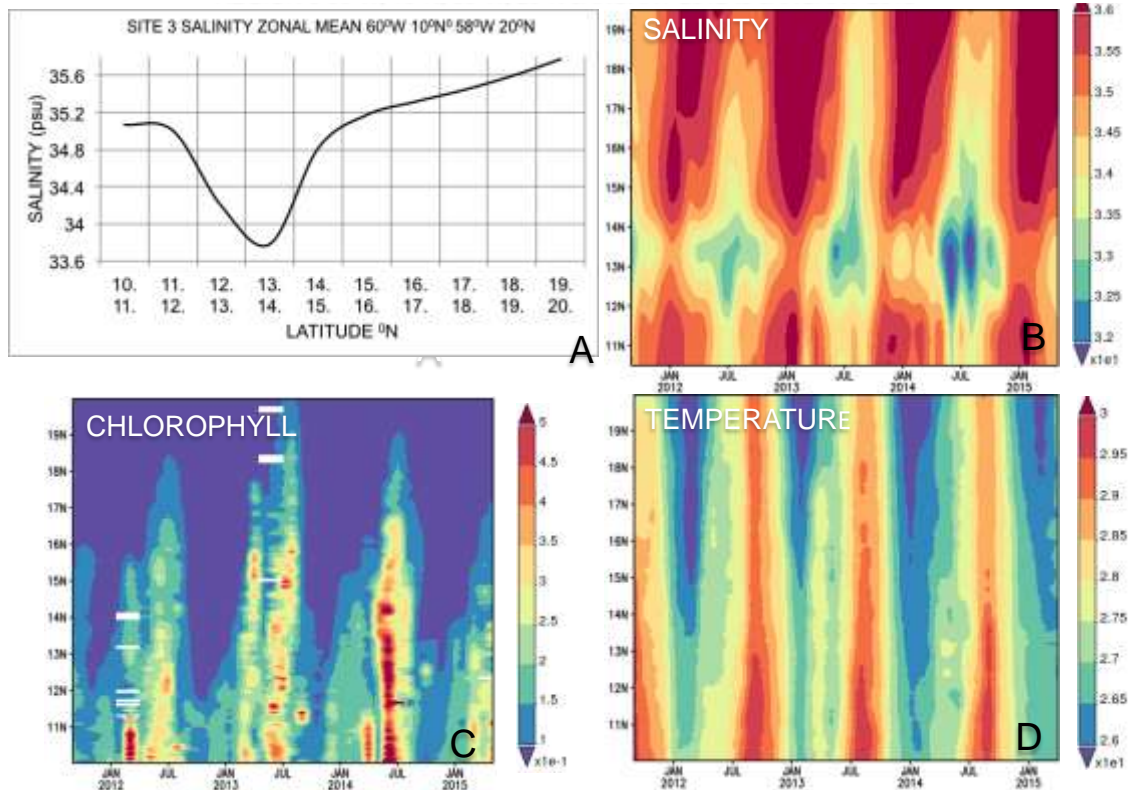


Figure 16: Observations in Site 3 at 10°N, 60°W to 20°N, 58°W, 2012 to 2015. A: Zonal mean of salinity; B: Hovmöller longitude averaged salinity; C: Hovmöller longitude averaged chlorophyll concentrations (mg m^{-3}); D: Hovmöller longitude averaged temperature ($^{\circ}\text{C}$). In comparing the figures, note the spatial resolutions of salinity at 100km while temperature and chlorophyll data are displayed at resolution of 4km (Giovanni).

The seasonal cycle for of salinity, temperature and chlorophyll in Figure 16 shows strong anomalous fluctuations in salinity with minima occurring during the summer months and a center of freshened water at 13°N to 14°N. While the latitude averaged zonal mean for salinity in Figure 16A provides the average position of the major influx, the salinity in Figure 16B shows that freshened water arrives in pulses and covers a wider latitudinal range that can stretch from 11°N to 16°N for salinity < 33.5 psu. The northern area in Figure 16B is characterized by aperiodic inflow of water from the Atlantic with higher salinity and the corresponding distribution of chlorophyll and temperature is shown in Figure 16C and 16D. It is notable that two chlorophyll maxima occur of which the first develops at the beginning of the year and the second maximum coincides with the arrival of freshened surface water during summer.

In site 3, the zonal latitude means for temperature and chlorophyll show an almost linear change as a function of latitude that is presented in Figures 17A and B, whereas the concentration of chlorophyll increases linearly with increasing temperature; however, this relationship is reversed west of the passages of the Lesser Antilles as shown in Figure 18.

The northern part of Site 4 is similar in its temperature distribution as in Site 3, but the southern part is impacted by colder water from the upwelling region along the Venezuela coast that also leads to elevated chlorophyll concentrations when compared to Site 3. Seasonal and aperiodic fluctuations in salinity, temperature and chlorophyll are documented in more detail with time series in Figure 19 that cover the timeframe during which salinity data were available and shows a comparison of Site 3 and 4 with linear regressions that reveal significant changes in salinity, temperature and chlorophyll concentrations. The

Research Article (Open Access)

water east of the Lesser Antilles in Site 3 shows a slight increase in salinity whereas west of the Lesser Antilles the salinity values have no recognizable change.

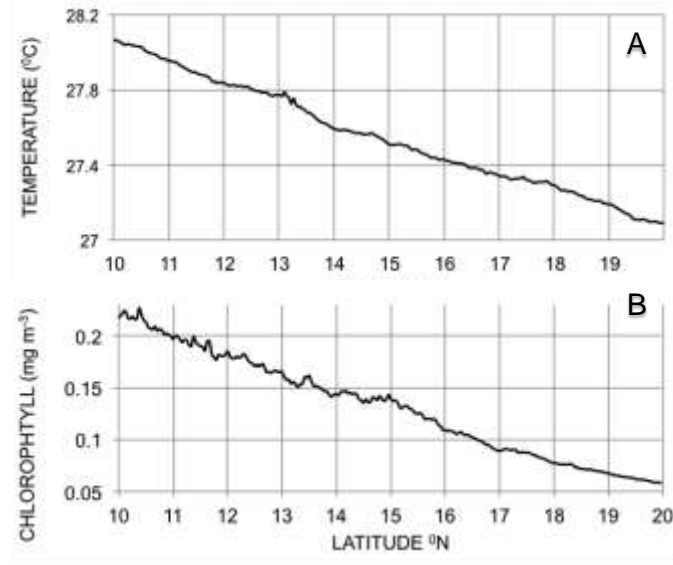


Figure 17: Zonal mean at Site 3 at 10°N, 60°W to 20°N, 58°W for September 2011 to May 2015. A: temperature (°C); B: chlorophyll (mg m⁻³); (Giovanni).

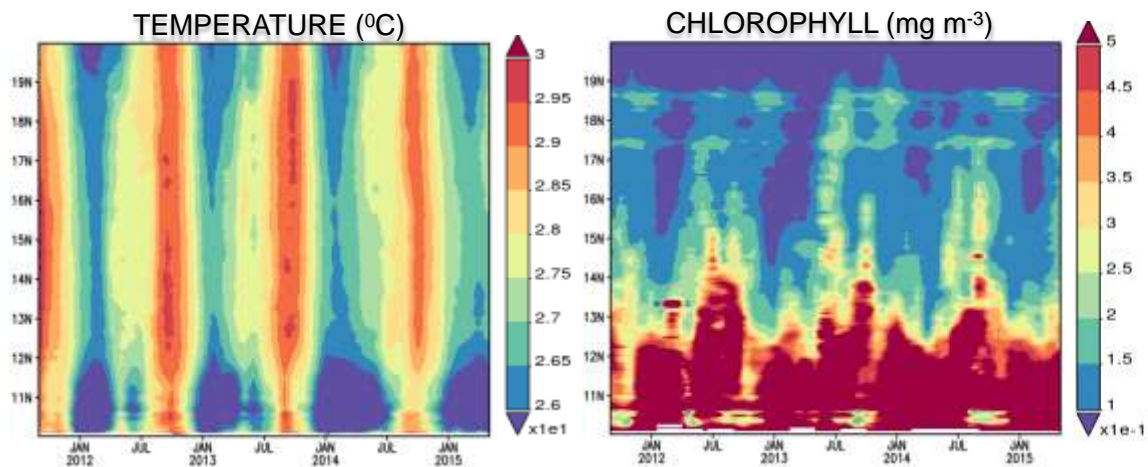


Figure 18: January 2012 To January 2015 Hovmöller longitude averaged temperature (°C) and chlorophyll (mg m⁻³) distribution for Site 4 at 10°N, 65°W to 20°N, 63°W (Giovanni)

The seasonal changes in Site 3 show that the water approaching the Lesser Antilles is about 0.3 psu lower in salinity as compared to Site 4. Both sites show an unusual but similar trend of decreasing temperature that is abnormal when compared to the level of global warming. Chlorophyll concentrations showed for both sides a slight increase although the main difference between the two sites is the concentration range of chlorophyll. Site 3 has a range from 0.08 to 0.3 mg m⁻³ while site 4 shows a concentration range from

Research Article (Open Access)

0.2 to 1.8 mg m⁻³, the latter being the result of advected upwelling water from the Venezuelan coast into the main current as is shown in Figure 18 with chlorophyll measurements.

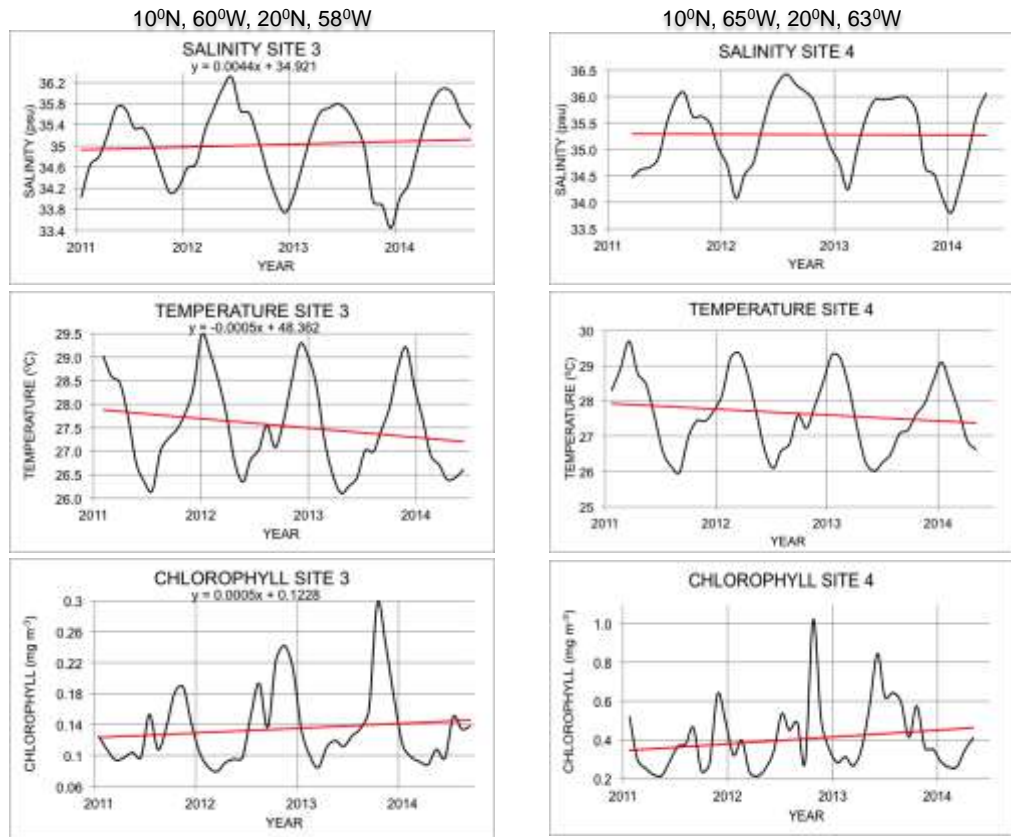


Figure 19: Comparison of time series for salinity, temperature and chlorophyll in Sites 3 at 10°N, 60°W to 20°N, 58°W and Site 4 at 10°N, 65°W to 20°N, 63°W (Giovanni).

To test if the observed trend is only a short-time pattern or presents a continuous long-term trend, all available temperature and chlorophyll data were analyzed for 2002 to 2022, but regrettably, salinity data were not available for this period. The results are shown in Figure 20 as time series with linear regressions and polynomial fits. The seasonal changes are distinct, but years with strong variations appear, especially with chlorophyll concentrations that show maxima that are not recognized after 2010. Furthermore, anomalous temperature signals were observed in 2009/2010 that coincided with chlorophyll anomalies interpreted as blooming events caused most probably by eddy activity, increased upwelling and higher river discharge.

Linear regression showed a decrease in temperatures as well as a decrease in chlorophyll concentrations. Based on the linear regression, the temperature decrease would correspond to cooling of about 0.04°C y⁻¹. However, the polynomial fit indicated that a process with a half-wavelength of ten years meanders through the region, and a similar conclusion can be derived from the change in chlorophyll concentrations.

The analysis of surface temperatures and chlorophyll concentrations in Figure 20 shows that the year 2010 was an anomaly. However, based on linear regression, water temperatures show a decrease of about 0.007°C y⁻¹. As small as this decrease is, it supports that the region at the entrance to the Caribbean Sea did not, for the time period analyzed, follow the general global trend in warming, and the explanation for this anomaly may be found in processes that are related to vertical advection of deeper water to the surface in

Research Article (Open Access)

the vicinity of the Lesser Antilles. The air temperature in the Lesser Antilles showed also a deviation from the global trend in warming that is documented in Table 1 with a summary of air temperature of the individual islands. Although a slight temperature increase is noted, the average change in air temperature for the Lesser Antilles is only around $0.0115\text{ }^{\circ}\text{C y}^{-1}$, whereas the estimate for Jamaica, shown for comparison, is about $0.0333\text{ }^{\circ}\text{C y}^{-1}$.

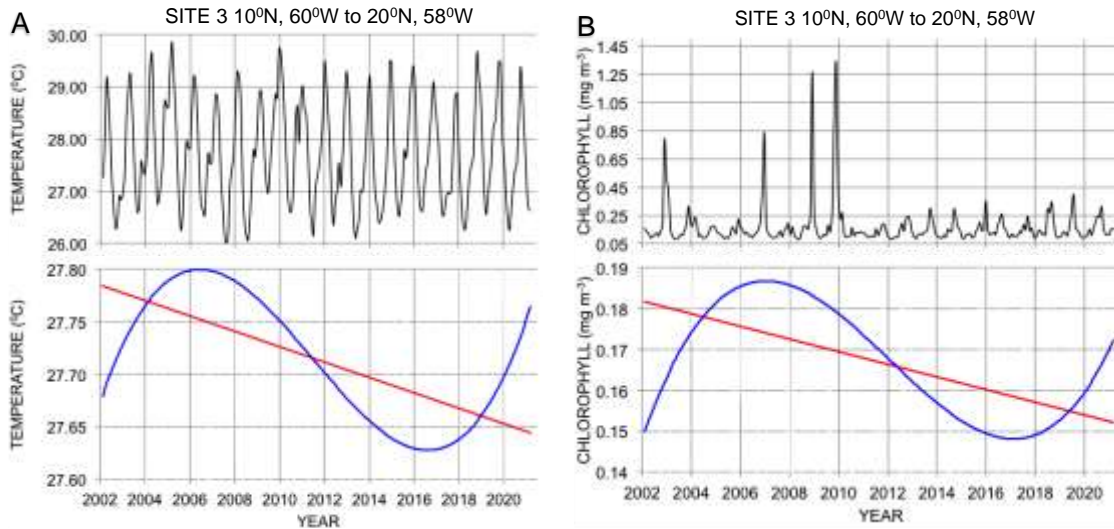


Figure 20: Comparison of temperature (A) and chlorophyll concentrations (B) in Site 3 at 10°N, 60°W to 20°N, 58°W. Red lines show linear regressions and blue lines show polynomial fits (Giovanni).

Table 1: Air temperature changes on the Lesser Antilles region in comparison to air temperature changes in Jamaica as calculated from www.meteoblue.com

ISLAND	1979	2021	$\Delta^{\circ}\text{C}$	$^{\circ}\text{C y}^{-1}$
Puerto Rico	23.9	24.7	0.8	0.0190
St Kitts/Nevis	25.8	26.3	0.5	0.0119
Montserrat	25.9	26.4	0.5	0.0119
Antigua	25.8	26.3	0.5	0.0119
Guadeloupe	25.3	25.8	0.5	0.0119
Martinique	25.8	26.2	0.4	0.0095
Dominica	25.7	26.1	0.4	0.0095
St. Lucia	26.2	26.8	0.6	0.0143
St. Vincent	26.1	26.5	0.4	0.0095
Grenada	26.2	26.7	0.5	0.0119
Tobago	25.9	26.3	0.4	0.0095
Trinidad	25.9	26.2	0.3	0.0071
Average	25.71	26.19	0.48	0.0115
Jamaica	24.5	25.9	1.4	0.0333

The measurements in Figure 19 and Figure 20 at the entrance to the Caribbean Sea do not allow for drawing conclusions for the whole Caribbean region, but observations in a selected region of the Columbia Basin in Figure 21 confirms that temperature anomalies around the Lesser Antilles were detected for 2011 to 2014 and also in the Columbia Basin with an increase in salinity and decrease in

Research Article (Open Access)

temperature. Compared to the waters around the Lesser Antilles, it can be assumed that waters in the Columbia Basin are well-mixed and therefore, it can be concluded that the anomaly signal was transferred through a larger part of the Caribbean Sea and adds to seasonal variations that are commonly observed (Fratantoni, 2001; Rueda-Roa and Müller-Karger, 2013; Jouanno and Sheinbaum, 2013).

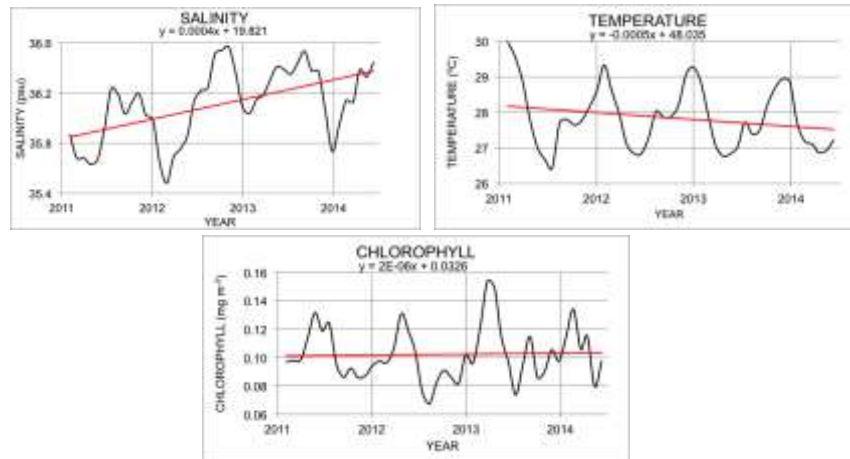


Figure 21: Salinity (psu), temperature ($^{\circ}\text{C}$) and chlorophyll (mg m^{-3}) concentrations for September 2011 to June 2015 for the central part of the Columbia Basin at 14°N , 80°W to 17°N , 75°W (Giovanni).

Although a negative temperature anomaly persists at the entrance of the Caribbean Sea after 2010, the effect of global warming is recognized with longtime series in the Columbia Basin as shown in Figure 22 although chlorophyll concentrations do not show any significant changes that would relate to the temperature anomalies. Linear regression emphasizes the changes of temperature with an increase of around $0.005^{\circ}\text{C y}^{-1}$ and a wavelength of about 15 years.

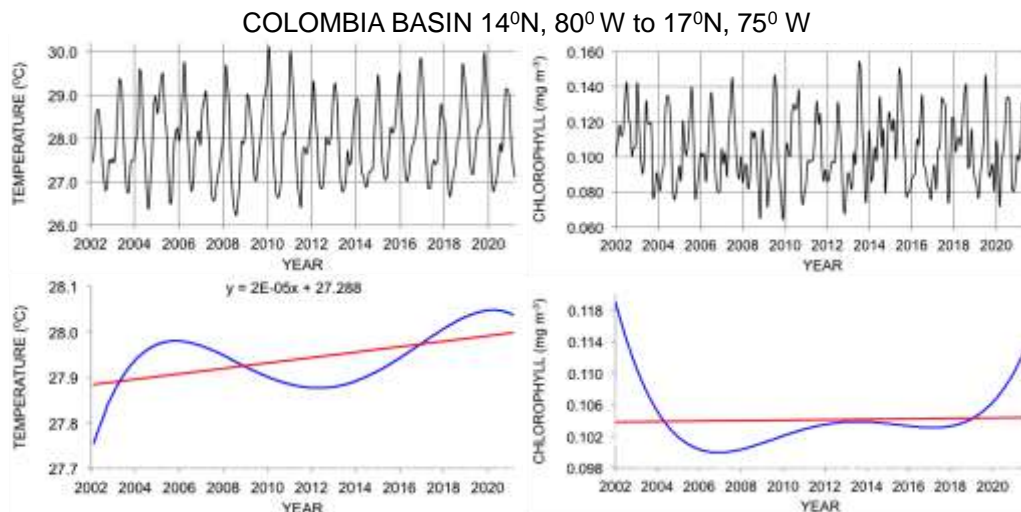


Figure 22: Temperature ($^{\circ}\text{C}$) and chlorophyll changes (mg m^{-3}) in the central part of the Columbia Basin in site 5 at 14°N , 80°W to 17°N , 75°W (Giovanni).

Chlorophyll concentrations in Figure 22 show seasonal fluctuations but linear regression does not indicate significant changes in concentrations. The observations on the relatively small changes in temperature in

Research Article (Open Access)

the investigated regions have to be viewed against the global change and from previous studies in the southern Caribbean Sea. Ecological changes in the southern Caribbean Sea between 1996 and 2010 document significant decadal scale trends with a net sea surface temperature rise of $\sim 1.0^{\circ}\text{C}$ and a standard deviation of $\pm 0.14^{\circ}\text{C}$ and as pointed out by Taylor et al. (2012), related to the warming trend are intensified stratification of the water column, reduced delivery of upwelled nutrients to surface waters and phytoplankton bloom decline.

CONCLUSIONS

The fluctuations in the Caribbean Sea indicate that Atlantic multi-decadal oscillations may be responsible for temporal and regional temperature variability. Variability of temperature either in the water or on islands is observed with anomalies and oscillations with long periods as indicated by polynomial regression of the data. Selected sites in Caribbean Sea revealed the regional differences in the dynamics of the Caribbean Sea and show that the intensity of regional oceanic processes need to be taken into account in considering air and sea surface changes. The Caribbean Sea is unique in that its salinity is mainly a result of periodic freshwater supply from the Amazon and Orinoco rivers through the channels of the Lesser Antilles. The retroflexion of the North Brazil Current and ring propagations, however, were seen to be major factors in transporting freshened water from the Amazon to the Caribbean Sea. Tracking of the freshened water revealed that the water enters through the Lesser Antilles passages in discrete packages and may reconstitute after the passage into organized anticyclonic movements with westward propagation.

Around 2010, an anomaly was observed with minimal sea surface temperature increase and even a negative deviation from the global warming trend was observed, in particular, in the region of the Lesser Antilles. Long-time series showed, however, that 2010 might have been an anomaly, as afterwards, the temperatures continued to increase. The anomalous period may have also been a phase of unusual ring activity in the Caribbean Sea as has been shown with analyses of sea surface height, salinity and temperature measurements. However, the overall agreement is that regional trends in sea surface temperature in the Caribbean Sea after 2010 continued to increase throughout the region. Average sea surface temperature for the wider Caribbean Sea is around $0.020^{\circ}\text{C y}^{-1}$ and may vary according to season from $0.017^{\circ}\text{C y}^{-1}$ to $0.024^{\circ}\text{C y}^{-1}$ (Glenn *et al.*, 2021), but as shown for the Lesser Antilles, a decrease of about $0.007^{\circ}\text{C y}^{-1}$ was observed. With the rather limited data set used in this study, it is difficult to address any quantitative forecast, especially in considering that the combined land and ocean temperatures have increased at an average rate of $0.008^{\circ}\text{C y}^{-1}$ since 1880, but the average rate of increase since 1981 has been even more than twice that rate (NOAA, 2021). Taking into account the long periodicity in environmental changes that were analyzed for the Caribbean Sea, especially with data documented in Figures 20 and 22, it is worthwhile to elaborate further on separating natural fluctuations from the anthropogenic signals in the Caribbean Sea at temporal scale of decades.

ACKNOWLEDGEMENTS

The author is affiliated with Columbia University EEC as Research Associate and is a Fulbright Alumnus and International Faculty Member at the Ateneo University de Manila, Department of Environmental Science (DES). The research was conceptualized at the University of The Bahamas in the Department of Applied Physics as a Fulbright Scholar 2017 to 2018. Images that are identified as IASNF in the text are from the Naval Research Laboratory - Ocean Sciences Division at https://www7320.nrlssc.navy.mil/IASNFS_WWW/IAS24.html; the permission to use them is gratefully acknowledged. The analyses and visualizations used in this study were produced with the Giovanni online data system, developed and maintained by the NASA GES DISC. The MODIS mission scientists and associated NASA personnel are acknowledged for the production of the data used in this research effort.

REFERENCES

- Acker JG and Leptoukh G (2007)**. Online Analysis Enhances Use of NASA Earth Science Data, *Eos Transactions American Geophysical Union*, **88**(2) 14-17.
- Andrade CA and Barton ED (2000)**. Eddy development and motion in the Caribbean Sea. *Journal of Geophysical Research*, **105** 26191-26201.
- Beier E, Bernal G, Ruiz-Ochoa M, Barton ED (2017)**. Freshwater exchanges and surface salinity in the Colombian Basin, Caribbean Sea. *PLoS ONE*, **12**(8) e0182116. <https://doi.org/10.1371/journal.pone.0182116>
- Carnes MR, Fox DN, Rhodes RC and Smedstad OM (1996)**. Data assimilation in a North Pacific Ocean monitoring and prediction system. In: *Modern Approaches to Data Assimilation in Ocean Modeling*, edited by Malanotte-Rizzoli, P, Elsevier Publishing. 455 pp.
- Carton JA and Chao Y (1999)**. Caribbean Sea eddies inferred from TOPEX/ POSEIDON altimetry and a 1/6 Atlantic Ocean model simulation. *Journal of Geophysical Research*, **104** C4, 7743–7752.
- Chérubin LM and Garavelli L (2016)**. Eastern Caribbean circulation and island mass effect on St. Croix, US Virgin Islands: A mechanism for relatively consistent recruitment patterns. *PLoS ONE*, **11**(3) e0150409. <https://doi.org/10.1371/journal.pone.0150409>
- Chérubin LM and Richardson PL (2007)**. Caribbean current variability and the influence of the Amazon and Orinoco freshwater plumes. *Deep Sea Research Part I: Oceanographic Research Papers*, **54**(9) 1451-1473. DOI: [10.1016/j.dsr.2007.04.021](https://doi.org/10.1016/j.dsr.2007.04.021)
- Chu PC, Wang G and Chenwu F (2004)**. Evaluation of the U.S. Navy's Modular Ocean Data Assimilation System (MODAS) Using South China Sea Monsoon Experiment (SCSMEX) Data. Naval Ocean Analysis and Prediction Laboratory, Department of Oceanography, Naval Postgraduate School, Monterey, CA 93943, USA 45 pp.
- Duncan CP, Schladow SG and Williams WG (1982)**. Surface currents near the greater and Lesser Antilles. *International Hydrographic Review*, Monaco, LIX 2 67- 78.
- Fox DN, Teague WJ, Barron CN, Carnes MR and Lee CM (2002)**. The Modular Ocean Data Assimilation System (MODAS). *Journal of Atmospheric and Oceanic Technology*, **19** 240–252. doi: [https://doi.org/10.1175/1520-0426\(2002\)019<0240:TMODAS>2.0.CO](https://doi.org/10.1175/1520-0426(2002)019<0240:TMODAS>2.0.CO).
- Frantantoni DM (2001)**. North Atlantic surface circulation during the 1990's observed with satellite-tracked drifters. *Journal of Geophysical Research*, **106** 22067-22093.
- Frantantoni DM and Richardson PL (2006)**. The evolution and demise of North Brazil Current rings. *Journal of Physical Oceanography*, **36** 1241-1264.
- Fu L-L and Holt B (1983)**. Some examples of oceanic mesoscale eddies by the Seasat synthetic aperture radar. *Journal of Geophysical Research*, **88**1844-1852.
- Garzoli S, Field A and Yao Q (2003)**. North Brazil Current rings and the variability in the latitude of retroflection. In: *Interhemispheric Water Exchange in the Atlantic Ocean*, edited by Goni G and Malanotte-Rizzoli P, *Elsevier Oceanography Series*, Elsevier, Amsterdam, **68** chap. 14, 357–374.
- Glenn E, Smith TM, Gálvez JM, Davison M, Hibbert K and González JE (2020)**. Tropical convection in the Caribbean and surrounding region during a regional warming sea-surface temperature period, 1982–2020. *Hydrology* **8** 56. <https://doi.org/10.3390/hydrology8020056>.
- Gómez Gaspar A and Acero A (2020)**. Comparison of the upwellings of the Colombian Guajira and eastern Venezuela. *Boletín de Investigaciones Marinas y Costeras – INVEMAR* **49**(2) Santa Marta. doi.org/10.25268/bimc.invemar.2020.49.2.943.
- Gordon AL (1967)**. Circulation of the Caribbean Sea. *Journal of Geophysical Research*, **72** 6207-6223.
- Gyory J, Mariano AJ and Ryan EH (2009)**. The Caribbean Current. *Ocean Surface Currents*. <https://oceancurrents.rsmas.miami.edu/caribbean/caribbean.html>.
- Hellweger FL and Gordon AL (2002)**. Tracing Amazon River water into the Caribbean Sea. *Journal of Marine Research*, **60** 537–549.
- Hu C, Montgomery ET, Schmitt RW and Müller-Karger FE (2004)**. The dispersal of the Amazon and Orinoco River water in the tropical Atlantic and Caribbean Sea: Observation from space and S-PALACE

Research Article (Open Access)

floats. *Deep-Sea Research Part II Topical Studies in Oceanography*, **51** (10-11) 1151-1171
DOI:10.1016/j.dsr2.2004.04.001.

Jochumsen, Rhein M, Hüttl-Kabus S, and Böning CW (2010). On the propagation and decay of North Brazil Current rings, *Journal of Geophysical Research*, **115** C10004, doi:10.1029/2009JC006042.

Johns WE, Townsend TL, Fratantoni DM and Wilson WD (2002). On the Atlantic inflow to the Caribbean Sea. *Deep-Sea Research, Part I*, **49** 211-243.

Jouanno J and Sheinbaum J (2013). Heat balance and eddies in the Caribbean upwelling system. *Journal of Physical Oceanography*, **43** 1004-1014. doi: 10.1175/JPO-D-12-0140.1.

Ko DS, Martin PJ, Rowley CD and Preller RH (2008). A real-time coastal ocean prediction experiment for MREA04. *Journal of Marine Systems*, **69** 17–28. doi:10.1016/j.jmarsys.2007.02.022.

Ko DS, Preller RH and Martin PJ (2003). An experimental real-time Intra Americas Sea Ocean Nowcast/Forecast System for coastal prediction. *Proceedings, AMS 5th Conference on Coastal Atmospheric and Oceanic Prediction and Processes*, 97–100.

Martin PJ (2000). Description of the Navy Coastal Ocean Model Version 1.0, Technical Report NRL/FR/7322-00-9962, 42 pp.

Morrison JM and Nowlin WD Jr. (1982). General distributions of water masses within the eastern Caribbean Sea during winter of 1972 and fall of 1983. *Journal of Geophysical Research*, **87** C6, 4207-4229.

Müller-Karger FE, McClain CR, Fisher TR, Esaias WE and Varela R (1989). Pigment distribution in the Caribbean Sea: Observations from space. *Progress in Oceanography*, **23** 23- 64.

Müller-Karger FE, McClain CR and Richardson PL (1988). The dispersal of the Amazon's water. *Nature*, **333** 56–59.

NOAA (2021). <https://www.climate.gov/news-features/understanding-climate/climate-change-global-temperature>

Nurse, LA, McLean RF, Agard J, Briguglio LP, Duvat-Magnan V, Pelesikoti N, Tompkins E and Webb A (2014). Small islands. In: *Climate Change 2014: Impacts, Adaptation, and Vulnerability. Part B: Regional Aspects. Contribution of Working Group II to the Fifth Assessment Report of the Intergovernmental Panel on Climate Change* edited by Barros, VR, Field CB, Dokken DJ, Mastrandrea MD, Mach KJ, Bilir TE, Chatterjee, M, Ebi KL, Estrada YO, Genova RC, Girma B, Kissel ES, Levy AN, MacCracken S, Mastrandrea PR, and White LI, Cambridge University Press, Cambridge, United Kingdom and New York, NY, USA 1613-1654.

Nystuen JA and Andrade CA (1993). Tracking mesoscale ocean features in the Caribbean Sea using Geosat altimetry. *Journal of Geophysical Research*, **98** 8389–8394.

Odriozola AL, Varela R, Hu C, Astor Y, Lorenzoni L and Müller-Karger FE (2007). On the absorption of light in the Orinoco River plume. *Continental Shelf Research*, **27** 1447–1464. doi:10.1016/j.csr.2007.01.012.

Palanisamy H, Becker M, Meyssignac B, Henry O and Cazenave A (2012). Regional sea level change in the Caribbean Sea since 1950. *Journal of Geodetic Science*, <https://doi.org/10.2478/v10156-011-0029-4>

Poveda GP Waylen R, and Pulwarty RS (2006). Annual and inter-annual variability of the present climate in northern South America and southern Mesoamerica. *Palaeogeography, Palaeoclimatology, Palaeoecology*, **234** (1) 3-27.

Restrepo JD and Kjerfve B (2000). Magdalena River: Interannual variability (1975–1995) and revised water discharge and sediment load estimates. *Journal of Hydrology*, **235** 137–149.

Richardson PL (2005). Caribbean Current and eddies as observed by surface drifters. *Deep-Sea Research II*, **52** 429–463.

Rowley C, Barron C, Smedstad L, and Rhodes R (2002). Real-time ocean data assimilation and prediction with GobaL NCOM. Naval Research Laboratory, Stennis Space Center. 0-7803-7535-1 IEEE, 775 -780.

Research Article (Open Access)

Rueda-Roa DT and Müller-Karger FE (2013). The southern Caribbean upwelling system: Sea surface temperature, wind forcing and chlorophyll concentration patterns. *Deep-Sea Research I*, **78** 102–114. <http://dx.doi.org/10.1016/j.dsr.2013.04.008>.

Schmitz WJ and Richardson PL (1991). On the sources of the Florida Current. *Deep-Sea Research Part A*, **38** (Suppl.), 379-409.

Stephenson TS, Vincent LA, Allen T et al. (2014). Changes in extreme temperature and precipitation in the Caribbean region, 1961–2010. *International Journal of Climatology*, Wiley Online Library (wileyonlinelibrary.com) DOI: 10.1002/joc.3889.

Taylor GT, Müller-Karger FE, Thunell RC, Scranton MI, Astor Y, Varela R et al. (2012). Ecosystem responses in the southern Caribbean Sea to global climate change. *Proceedings of the National Academy of Sciences of the United States of America*, **109** 47 19315-19320; <https://doi.org/10.1073/pnas.1207514109>

Torres RR and Tsimplis MN (2012). Seasonal sea level cycle in the Caribbean Sea. *Journal of Geophysical Research Oceans*: **117** Issue C7. <https://doi.org/10.1029/2012JC008159>.

Van der Boog CG, Pietrzak JD, Dijkstra HA, Brüggemann N, van Westen RM, James RK, Bouma TJ, Riva REM, Slobbe DC, Klees R, Zijlema M, and Katsman CA (2019). The impact of upwelling on the intensification of anticyclonic ocean eddies in the Caribbean Sea. *Ocean Science*, **15** 1419–1437. <https://doi.org/10.5194/os-15-2019>.

Copyright: © 2022 by the Author, published by Centre for Info Bio Technology. This article is an open access article distributed under the terms and conditions of the Creative Commons Attribution (CC BY-NC) license [<https://creativecommons.org/licenses/by-nc/4.0/>], which permit unrestricted use, distribution, and reproduction in any medium, for non-commercial purpose, provided the original work is properly cited.